Transportation Research Part C 163 (2024) 104615

Contents lists available at ScienceDirect

Transportation Research Part C

journal homepage: www.elsevier.com/locate/trc

Sustainable last-mile distribution with autonomous delivery robots and public transportation☆

Annarita De Maio [a], Gianpaolo Ghiani [c], Demetrio Laganà [b], Emanuele Manni [c,*]

[a] Department of Economics, Statistics and Finance "Giovanni Anania" - DESF, University of Calabria, Rende, Italy
[b] Department of Mechanical, Energy and Management Engineering - DIMEG, University of Calabria, Rende, Italy
[c] Department of Engineering for Innovation, University of Salento, Lecce, Italy

ARTICLE INFO

Keywords:
Last-mile distribution
Multimodal transportation
Autonomous delivery robot routing and scheduling
Destroy-and-repair

ABSTRACT

In recent years, the rapid growth of e-commerce and the need to make last-mile logistics more sustainable have stimulated the development of new distribution paradigms, based on air drones and autonomous delivery robots, which are less sensitive to traffic congestion. In this article we deal with a routing problem in which a fleet of autonomous delivery robots can travel not only on the road network but also on the public transportation system (or part of it) to extend their range of action with a given battery capacity. The problem entails building delivery robot routes synchronized with the rides of the public transportation lines, enabling robots to drop on/off public vehicles, where they use dedicated compartments, to reach customers that would be otherwise out of reach. To this purpose, we develop a tailored destroy-and-repair mechanism that, embedded into a neighborhood search algorithm, allows to effectively explore the feasibility region of large-scale instances. Extensive computational results on instances resembling the distribution of drugs to pharmacies in Rome (Italy) show that the proposed algorithmic mechanism allows to obtain a cost reduction up to about 7.5% with respect to a more traditional approach. Moreover, from a managerial point of view, our experiments show that autonomous delivery robots combined with public transportation can provide huge benefits in terms of costs and emissions reduction, when compared to both traditional and electric vans.

1. Introduction

In recent years, the rapid growth of the e-commerce sector and the increase in express deliveries have generated a growing traffic congestion in urban areas and, consequently, a worrying rise in CO_2 emissions and other pollutants. Indeed, this trend is expected to grow: total e-commerce sales are estimated to increase to about 3 trillion euros by 2023 (Statista, 2023), with significant volumes of parcel deliveries moving within cities. The debate on the *sustainable development goals* (SDGs) introduced by the 2030 Agenda (United Nations, 2022) has stimulated a number of *green logistics* initiatives that have the potential to reduce waste and improve energy efficiency (zero hunger and clean and affordable energy SGDs), diminish air pollutant emissions and related health impacts (good health and well-being SGD), and play a key role in climate resilience (climate action SGD).

To mitigate the impact of last-mile logistics, several relevant innovations have been introduced in the past decade based on new information and communication technologies as well as on robotics. These innovations have the potential to increase efficiency

☆ This article belongs to the Virtual Special Issue on "Transport Logistics".

* Corresponding author.
E-mail addresses: annarita.demaio@unical.it (A. De Maio), gianpaolo.ghiani@unisalento.it (G. Ghiani), demetrio.lagana@unical.it (D. Laganà), emanuele.manni@unisalento.it (E. Manni).

https://doi.org/10.1016/j.trc.2024.104615
Received 1 July 2023; Received in revised form 9 April 2024; Accepted 9 April 2024

Fig. 1. Autonomous delivery robots examples. From left to right: Starship's robot, Aramex's bot, FedEx Roxo SameDay Bot.

and reduce logistics costs (economic growth SGD), improve intermodal exchanges (industry, innovation and infrastructure SGD) and optimize vehicle mileage (sustainable cities and communities SGD) *by redistributing a portion of freight to non-motorized modes and public transport* (Sehlleier et al., 2017). Ranieri et al. (2018) have classified them into several categories: new automated vehicles (Alonso Raponso et al., 2022), proximity hubs (e.g., cargo-bike micro hubs and delivery lockers, see Grabenschweiger et al., 2021; Carracedo and Mostofi, 2022), collaborative and cooperative urban logistics (e.g., crowdshipping solutions, see Le et al., 2019). Chen et al. (2021) have estimated that the usage of automated vehicles could be a reasonable solution for 80% of all the last-leg deliveries in the near future. In fact, several companies, such as DHL, UPS, or Amazon (see Vincent and Gartenberg, 2019; Macrina et al., 2020) have already experimented the use of unmanned aerial vehicles (UAVs) in real-world settings. However, factors like flying regulations, low cost competitiveness and low transport capacity limit the use of this technology. This stimulated the use of a new generation of drones (autonomous delivery robots or unmanned ground vehicles or self-driving robots, ADRs) to perform deliveries in the highly congested urban areas of the megacities (Bailey, 2016). This innovation has become less futuristic after the Covid-19 pandemic (see Kapser et al., 2021; Pani et al., 2020), where the need for social distancing has led to an increase in research and investments in this field. Nowadays, different companies are developing pilot initiatives for testing ADRs: for example, Starship Technologies is running a self-driving robot service in the city of London (Starship, 2020), as well as e-Novia and Twinswheel in different cities (Chen et al., 2021). Recently, Aramex launched a self-driving delivery robot (Geronimo, 2023), while FedEx experimented its six-wheeled autonomous delivery robot, called Roxo SameDay Bot (FedEx, 2020). Some examples of autonomous delivery robots are depicted in Fig. 1.

From a technological perspective, the main difference between ADRs and UAVs is related to their autonomy and speed, as well as to their feasible payloads. UAVs are usually able to travel at a faster speed than ADRs, but the number of ADRs that can be transported on an auxiliary vehicle (e.g., a truck) is usually greater than the number of UAVs. These aspects, combined with the fact that not always a landing area is available in densely-populated cities, explain why UAVs are typically used to perform deliveries in rural areas, while ADRs are considered advantageous in urban last-mile delivery. Indeed, self-driving delivery robots can provide a relatively cheap and sustainable solution to the current last-mile logistics challenge, as well as they can deliver small packages reaching the customer doors using sidewalks, while traveling at relatively low speeds to satisfy safety requirements (Chen et al., 2021). Efficient solutions have also been devised through the use of ADRs in synergy with other vehicles, such as trucks, like in the paradigm known as *truck-and-robot delivery* (Boysen et al., 2018; Yu et al., 2022). One possible application comes from the partnership between Mercedes-Benz and Starship Technologies. This alliance consists in developing a truck-based robot delivery concept called Robovan, i.e., a modified van designed to move Starship's robots around cities. This allows the ADRs to be transported to a predefined drop-off point, where they are unloaded and move independently to make deliveries. Once the deliveries are made, the ADRs reach an intermediate depot, where the van will retrieve them. For more examples of applications of the truck-and-robot delivery paradigm, the reader is referred to Chen et al. (2021), Alfandari et al. (2022), Heimfarth et al. (2022) and Kloster et al. (2023). A discussion of the potential of ADRs can be found in Lemardelé et al. (2021), while a comprehensive overview of the role played by ADRs in city logistics is discussed in Kunze (2016), Srinivas et al. (2022) and Alverhed et al. (2024).

Another promising opportunity is to combine freight transportation with Public Transportation (PT): for example, spare capacity in buses or taxes can be used for transporting small parcels around specific zones of the urban areas. Although this latter opportunity could create evident benefits such as - among others - reducing road congestion and, as a consequence, air pollution, the integration of these two transportation modes has been limited to a few experiments (Masson et al., 2017), mainly involving freight being transferred from traditional vehicles onto PT vehicles.

In our work, we combine these aspects from a different perspective and consider a problem arising in a city-logistics context in which a fleet of ADRs is used to service a set of requests in an urban area. In our problem, we assume that the delivery robots can autonomously ride on PT vehicles (e.g., bus, train, or metro) as part of their routes to reach customers that otherwise would have been too far, because of the limited robot battery duration. The goal is to find a set of routes of minimum total cost, such that each daily request is served by exactly one vehicle. The robot routes must fulfill all the operational constraints related to their capacity, the distance that they can cover with a fully-charged battery when traveling on the streets, as well as the synchronization between their arrival times at the stops of the public lines with the scheduled departure and arrival times of these lines, to avoid unnecessary waiting. In the following, the problem is referred to as the *Autonomous Delivery Robot Routing Problem with Public Transportation* (ADRRPT). Although similar problems have been addressed in the scientific literature (as will be highlighted in Section 2), our

innovative contribution is the design of an algorithm capable of solving large instances of the problem by exploiting its geographical features. Specifically, our main contributions can be summarized as follows. Firstly, we present a mathematical formulation of the ADRRPT, where the goal is to minimize the total time traveled by the ADRs by accounting for a multimodal logistics system. This system includes the time ADRs take to travel along the pedestrian network, serve customers, reach a public service line stop, wait for the arrival of the scheduled transport line, travel on the line, and return to the depot. The computation of these times implicitly considers the synchronization between the robots' arrival at the stops and the time of the lines. This is a crucial factor for evaluating the performance of the proposed algorithm. Secondly, we design a metaheuristic solution strategy in which destroy-and-repair operations are coordinated to explore efficiently the feasibility region of the problem. The proposed mechanism exploits the geographical structure of the public transport lines through a propagation effect, which can help to improve the solution quality. Thirdly, we perform a thorough computational study on a set of realistic large-scale instances with up to 500 customers, resembling the distribution of medicines to pharmacies in the urban area of Rome (Italy). Finally, we derive important managerial insights showing the benefits of using the proposed delivery infrastructure of ADRs combined with the PT network, in terms of both costs and emissions reduction, when compared to more traditional delivery schemes.

The remainder of the paper is organized as follows: Section 2 reports an overview of the related literature, Section 3 provides the problem description, and Section 4 introduces a metaheuristic for solving the problem. Then, Section 5 describes the computational results, followed by conclusions in Section 6.

2. Literature review

In this section we present an overview and comparative analysis of the main scientific literature related to our work. We focus on recent developments in drone routing problems and freight delivery in combination with public transportation. Freight delivery exploiting the public transportation system has received increasing attention during the last decade as a result of government incentives in several industrialized countries and, in particular, in the European Community. Various contributions aim to exploit the synergies between freight and passenger flows in urban areas. This class of problems is often referred to as *Freight-on-Transit* problems (see Delle Donne et al., 2023), with a distinction between *single-tiered* and *two-tiered* systems (Mourad et al., 2019). In single-tiered systems, vehicles move passengers and freight simultaneously subject to a variety of operational constraints, such as those related to time windows and vehicle capacities (see Li et al., 2014; Archetti et al., 2016). In this respect, recently Bosse et al. (2023) propose an integration of on-demand passenger and goods transportation services. They employ a centralized anticipatory-optimization approach for passenger-freight combination, which - as they show - has significant potential for improving transportation efficiency. In contrast to the issue discussed by Bosse et al. (2023), our work focuses on robots delivering goods using both pedestrian and public transportation networks. In two-tiered systems (Cochrane et al., 2017; Behiri et al., 2018), a public transportation system is used for moving freight (first tier), while last-mile deliveries to customers are performed with (possibly electric) vans, cargo bikes, etc. (second tier). Within this research area, Kızıl and Yıldız (2023) introduce a framework that utilizes public transport as the primary network, supported by automated service points, crowd-shipping, and zero-emission vehicles to complete deliveries in a cost-efficient and environmentally-friendly manner. Azcuy et al. (2021) aim to identify the most suitable transit stop, within a single transit line, to serve as a transfer location in a two-tier system. The study reveals potential cost savings resulting from this integration to support urban delivery. Comprehensive surveys of these problems are presented in Galkin et al. (2019), Elbert and Rentschler (2022) and Delle Donne et al. (2023).

Hörsting and Cleophas (2023) introduce a comprehensive evaluation of the benefits of employing PT networks through simulation techniques. The authors analyze the integration of freight transportation via trams and metros, taking into account two primary scenarios, namely shared infrastructure mode whereby both freight and passenger services have a designated capacity, and shared vehicle mode, whereby capacity is assigned based on the actual passenger flow. This study illustrates that a system utilizing shared vehicles is more resilient to changes in demand, whereas a system relying uniquely on shared infrastructure presents a viable solution for managing idle times of vehicles transporting goods. Although the transportation of goods using public transport, such as in two-tiered systems, may appear similar to our problem, still there are significant differences. In particular, in our problem, robots are fully dedicated to the transportation of goods, and they get on and off the public transport to reach distant locations that cannot be visited directly due to the limited distances they can travel with a full battery.

Thanks to recent technological advancements in electric and autonomous vehicles, there is a growing interest in combining their distribution capabilities with public transport routes. In this regard, a literature review on the opportunities and challenges of freight transportation via public transport networks is presented by Rong Cheng and Nielsen (2023), who identify a gap in the literature on the potential use of UAVs and ADRs in conjunction with public transport. The authors emphasize the need for a thorough study of the impacts of such a synergistic system before a widespread application. To the best of our knowledge, the only contributions devoted to last-mile delivery with ADRs combined with public transportation are due to Mourad et al. (2021) and Ermagan et al. (2023). Concerning Mourad et al. (2021), peculiar features of this contribution are: delivery robots can carry unit loads; passengers and robots share the PT capacity; PT trips are modeled as direct connections between their origin–destinations stations. For this problem, the authors propose a scenario-based Sample Average Approximation (SAA) combined with an Adaptive Large Neighborhood Search (ALNS) procedure to solve instances with up to 100 freight requests. On the other hand, Ermagan et al. (2023) study a pickup and delivery problem, in which delivery robots serve a set of dynamic requests, and are allowed to use more than one public transit vehicle. To optimize real-time operations, the authors introduce a rolling-horizon algorithm based on column generation. Our work differs from those of Mourad et al. (2021) and Ermagan et al. (2023) in several respects. The problem described by Mourad et al. (2021) involves a pickup and delivery scenario where ADRs can serve one request at a time by executing direct

or indirect deliveries based on their limited travel distance. In contrast, in our problem the ADRs can perform multiple deliveries with a single route. Moreover, the ADRs and passengers have separate capacities for travel (e.g., dedicated compartments), unlike what Mourad et al. (2021) assume. Moreover, Mourad et al. (2021) design a SAA method along with an ALNS algorithm to solve instances with up to 100 freight requests. The algorithm we design is capable of solving instances of the problem with a number of customers ranging from 100 to 500. In addition, we consider explicitly the sequence of stations visited by a PT vehicle which has some advantages when solving large-scale instances of the problem. Concerning the delivery system studied by Ermagan et al. (2023), it presents significant differences compared to ours as well. Specifically, Ermagan et al. (2023) study a dynamic problem involving a pickup and delivery station that may have multiple orders and be visited more than once by an ADR. In contrast, we do not account for the dynamism of the requests because in our application context the pharmacy orders are known a priori, and we allow each delivery location to be served by at most one ADR. Moreover, Ermagan et al. (2023) investigate different positioning policies to determine the optimal strategy for directing each ADRs to the appropriate hub to serve future customers upon completion of the service. Furthermore, these hubs allow for the recharging of ADRs. In our problem, each ADR returns to the same depot from which its route starts, where it can recharged (however, we do not take into account recharging issues). Additionally, Ermagan et al. (2023) assume the use of a backup delivery capacity provided by dedicated couriers when the ADRs' capacity is insufficient, while we do not use a third-party provider. In our problem the objective is to minimize the total travel time of the ADRs, rather than just the operational costs incurred by using ADRs and dedicated couriers as proposed in Ermagan et al. (2023). To address this problem, Ermagan et al. (2023) propose a rolling-horizon approach and develop a machine learning-enhanced column generation algorithm for a quick solution. On the other hand, we develop a metaheuristic algorithm that exploits geographical features of the public transportation lines.

3. Problem description and notation

In this section we describe and formalize the problem. We refer to an operational problem in which a fleet Δ of ADRs must serve a set of customers, starting and ending their routes from/at a depot (not necessarily the same for each ADR). Each ADR departs from its depot and can use the service lines of a PTN. According to Hörsting and Cleophas (2023), robots that board public transportation vehicles occupy a designated area that is reserved for freight. It is assumed that the area is sufficiently large to accommodate multiple ADRs and that there are no capacity constraints that would restrict the route plan. When an ADR arrives at a PT station, it can wait for the vehicle to arrive before boarding. The ADR will then get off at the PT station closest to the locations where the deliveries need to be made. The ADR can continue its route within the battery constraints and return to its depot. The ADRs do not consume battery power while traveling on the PT vehicle. Fig. 2 shows a graphic representation of the problem. More specifically, this figure illustrates how the ADRs synchronize and coordinate with the PT lines. Here, the ADRs depart from the depot, arrive at the most suitable PT stop, and board the PT vehicles. After reaching the scheduled PT destination stops, the ADRs deliver the required freight to the pharmacies according to their schedules and depart either from the same PT stop or the stop closest to the last visited pharmacy. It is important to note that this entire process is subject to synchronization constraints to minimize waiting times for the ADRs at PT stops. For instance, let us consider ADR1, i.e., the red route in Fig. 2. The delivery robot leaves the depot at 10:00am, and reaches the PT1 stop after five minutes (covering a distance of 0.5 km at a speed of 6 km/h). It then boards the vehicle at 10:08am, after a three-minute wait. Traveling through the PT network, ADR1 arrives at stop PT8 at 10:15am. Continuing its route, ADR1 reaches the first pharmacy at 10:21am, having covered a distance of 0.6 km in 6 minutes. After a service time of 4 minutes, ADR1 departs at 10:25am and travels for another 4 minutes to arrive at the second pharmacy, which is 0.4 km away. After spending another 4 minutes servicing the second pharmacy, ADR1 leaves at 10:33am. Finally, ADR1 travels 5 minutes to stop PT9, boards the PT vehicle after a 2 minute wait, and gets back at the depot at 10:55am after 10 minutes on the PT vehicle and 5 minutes on the road. To formalize the ADRRPT we refer to the notation reported in Table 1, which is used throughout the paper.

The ADRRPT is defined on a directed graph $G = (V, A)$, with $V = V_C \cup V_E$, where V_C is the set of nodes corresponding to the customer locations, and V_E is defined as follows. Let V_P denote the set of nodes of the PTN including the depot o_δ for each autonomous delivery robot $\delta \in \Delta$. Then, to model the Public Transportation Network (PTN) timetable in a time-expanded fashion we replicate each node of the PTN as many times as the number of arrivals/departures at/from it. Then, with each replicated node we associate a pair (original node, scheduled time), so that $V_E = \{o_1, \ldots, o_{|\Delta|}\} \cup_k \{i^k = (i, p_i^k)\}$, where, for pair (i, p_i^k), $i \in V_P$ and p_i^k is the kth scheduled arrival/departure time at/from i. To each node $i \in V$ is associated a service time s_i. Note that, for nodes $i \in V_E$, it represents the time needed for an ADR to get on/off a PT vehicle. This way of modeling the synchronization between autonomous delivery robots and scheduled public transport lines facilitates the analysis of the interactions between passengers and the transport network. If an ADR arrives at node (i, p_i^k) of a PT stop after p_i^k, it shall wait there until the next departure time. Otherwise, it shall drop onto the PT vehicle. Furthermore, with regards to the service time s_i at nodes $i \in V_E$, as noted by Ermagan et al. (2023), the ADRs considered in the ADRRPT can get on/off PT vehicles in a reasonable amount of time, having - in practice - no effect on the punctuality of the line schedule. All these considerations allow us to concentrate on the routing aspects of the ADRRPT, as outlined below. As far as the arc set is concerned, $A = A_E \cup A_C \cup A_L$, where $A_E = \{(i, j) : i, j \in V_E\}$ is the set of arcs connecting two vertices of the time-expanded PTN, $A_C = \{(i, j) : i, j \in V_C\}$ is the set of arcs connecting two customers, $A_L = \{(i, j) : (i \in V_C \wedge j \in V_E) \vee (i \in V_E \wedge j \in V_C)\}$ is the set of arcs connecting a customer to an element in V_E, or vice versa. With each arc $(i, j) \in A$ is associated a distance d_{ij} and a travel time t_{ij}. In particular, d_{ij} represents the distance between two nodes on the road network, which is set to 0 for arcs connecting two nodes corresponding to PTN stops, given that when a delivery robot travels on such arcs it does not consume its battery. In addition, t_{ij} is computed as follows. If $(i, j) \in A_E$, then t_{ij} is the scheduled travel time for a PT vehicle connecting i to j and leaving from i at a given scheduled time. If $(i, j) \in A_C \cup A_L$, then $t_{ij} = d_{ij}/v$, where

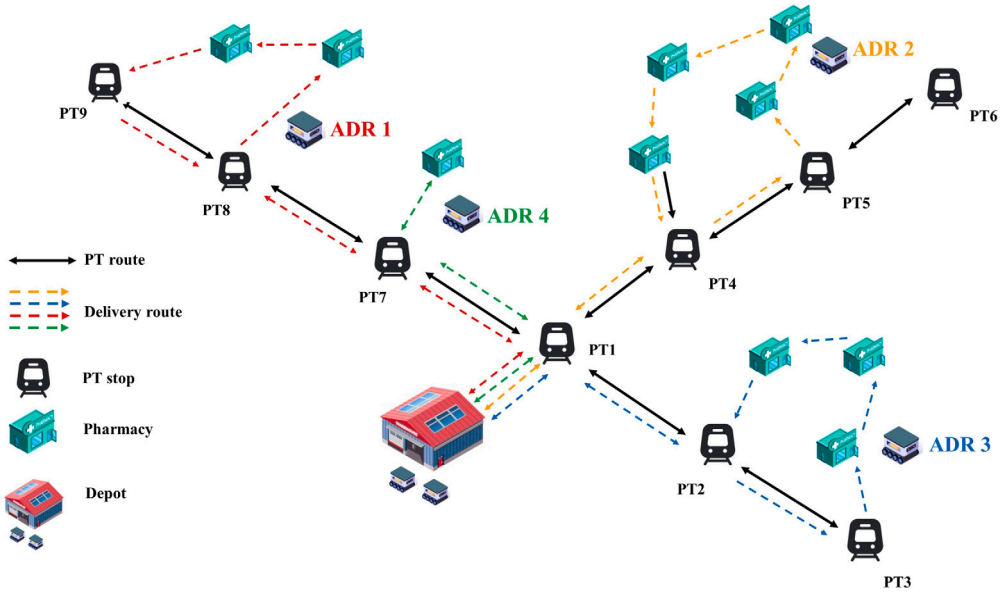

Fig. 2. A sample delivery plan for four ADRs exploiting the PTN.

Table 1
Overview of the notation used throughout the paper.

Δ	set of autonomous delivery robots
V_P	set of nodes of the PTN including the depot o_δ for each $\delta \in \Delta$
V_E	set of time-expanded nodes $i^k = (i, p_i^k)$
V_C	set of customer locations
V	set of all nodes, $V = V_C \cup V_E$
A_E	set of arcs connecting two vertices of the PTN
A_C	set of arcs connecting two customer locations
A_L	set of arcs connecting a customer location to a PTN stop (or vice versa)
A	set of all arcs, $A = A_E \cup A_C \cup A_L$
s_i	service time at node $i \in V$
d_{ij}	distance on arc $(i, j) \in A$
d_δ	the maximum distance that can be traveled by an autonomous delivery robot when it is fully charged
v	average speed at which autonomous delivery robots travel on the road network
t_{ij}	travel time on arc $(i, j) \in A$
q_i	demand of customer $i \in V_C$
Q_δ	capacity of autonomous delivery robot $\delta \in \Delta$

v is the average speed at which ADRs travel on the road network. In addition, each robot $\delta \in \Delta$ has a capacity Q_δ, defined in terms of storage compartments. This value must be taken into account when deciding the allocation of the customers, whose demand q_i, $i \in V_C$, is expressed as the number of robot compartments needed.

The main issues to address when solving the ADRRPT are:

- the allocation of customers to ADRs and, more specifically, deciding whether it is more convenient to service a request by using either an ADR only, or an ADR combined with one or more rides of PT vehicles;
- the construction of a set of ADR feasible routes that are synchronized with the scheduled lines of the PT vehicles. Each route starting at a depot and servicing all the customers at the minimum total cost (in terms of traveled distance), while fulfilling all the operational constraints related to the limited distances that can be traveled by the ADRs due to the battery duration as well as to their limited capacity. We note that ADRs do not need to be recharged when they arrive at PTN stops, because given that their battery usage is switched off whenever they are traveling along a PT line, the routes assigned to them can be fulfilled without the need for any further battery re-charging.

Further notation is required to mathematically formulate the ADRRPT. Specifically:

- $\Sigma(S)^+$, set of arcs outgoing $S \subseteq V_C$;
- $\Sigma(S)^-$, set of arcs incoming $S \subseteq V_C$;
- $\alpha(S)$, minimum number of delivery robots required to serve all the customers in $S \subseteq V_C$. If all ADRs have the same capacity Q, this parameter can be defined as $\lceil \sum_{i \in S} q_i / Q \rceil$;
- x_{ij}^{δ}, binary variable set to 1 iff autonomous delivery robot δ uses arc (i, j).

A binary formulation for the ADRRPT is:

$$\text{(F-ADRRPT)} \min \quad \sum_{\delta \in \Delta} \sum_{(i,j) \in A} t_{ij} x_{ij}^{\delta} \tag{1}$$

$$\text{s.t.} \quad \sum_{\delta \in \Delta} \sum_{i \in V} x_{ij}^{\delta} = 1, \qquad j \in V_C \tag{2}$$

$$\sum_{i \in V} x_{o_\delta i}^{\delta} \leq 1, \qquad \delta \in \Delta \tag{3}$$

$$\sum_{j \in V} x_{ij}^{\delta} - \sum_{j \in V} x_{ji}^{\delta} = 0, \qquad i \in V,\ \delta \in \Delta \tag{4}$$

$$\sum_{(i,j) \in A_C \cup A_L} d_{ij} x_{ij}^{\delta} \leq d_{\delta}, \qquad \delta \in \Delta \tag{5}$$

$$\sum_{i \in V_C} q_i \sum_{j \in V} x_{ij}^{\delta} \leq Q_{\delta}, \qquad \delta \in \Delta \tag{6}$$

$$\sum_{(i,j) \in \Sigma(S)^+ \cup \Sigma(S)^-} \sum_{\delta \in \Delta} x_{ij}^{\delta} \geq 2\alpha(S), \qquad S \subseteq V_C,\ |S| \geq 2 \tag{7}$$

$$x_{ij}^{\delta} \in \{0, 1\}, \qquad (i, j) \in A,\ \delta \in \Delta \tag{8}$$

The aim of objective function (1) is to minimize the total travel time. Constraints (2) guarantee that every customer is served exactly by a robot, whilst constraints (3) stipulate that a robot may leave depot only once. Constraints (4) ensure flow balance at every vertex and with each delivery robot. Constraints (5) guarantee that the distance covered by each robot's route does not exceed a specified threshold. Constraints (6) ensure that the maximum capacity of the robots is not exceeded. Constraints (7) correspond to the connectivity constraints and impose that the minimum number of arcs traversing the set S is at least twice the number of robots required to serve all the customers in S. Such constraints have a cardinality growing exponentially with $|V_C|$, and could be dynamically added to the mathematical formulation when a violation is detected within a branch-and-cut algorithm. Finally, constraints (8) define the domain of the variables.

The ADRRPT is $\mathcal{NP}$-hard since it is a generalization of the multi-depot capacitated vehicle routing problem with length constraints (Contardo and Martinelli, 2014). As a result, the (F-ADRRPT) is only suitable for solving small-sized instances of the problem, and heuristic or metaheuristic approaches are needed to tackle instances of practical size in a reasonable amount of time. In particular, the (F-ADRRPT) formulation is used to provide feasible solutions and valid lower bounds for comparison with the results obtained using the designed metaheuristic, as shown in Section 5.3.1.

4. A coordinated destroy-and-repair metaheuristic for the ADRRPT

In this section we present a detailed description of our metaheuristic approach to solve the ADRRPT. The basic idea is starting from a feasible solution and iteratively improving it by means of a neighborhood-search approach. At each iteration, a neighborhood of the current solution is explored by employing a new mechanism dubbed *Destroy-and-Repair Propagation* (DRP). DRP is then embedded into a Variable Neighborhood Descent (VND) framework (Duarte et al., 2018).

More specifically, the implemented VND explores neighborhoods of increasing size through a classical destroy-and-repair approach until a local optimum is encountered. At that point, the search process moves to a larger neighborhood trying to improve further. This is motivated by the evidence that if a candidate solution is locally optimal in a specific neighborhood, this is not guaranteed for another different neighborhood (Martí et al., 2018). Once the whole sequence of VND neighborhood structures has been explored without any solution improvement, a diversification phase (based on a random perturbation of the distances associated with the arcs of the graph) is invoked and the search process is then restarted and iterated until a predefined time limit is reached.

The general structure of our *coordinated destroy-and-repair* metaheuristic is depicted in Algorithm 1. The algorithm inputs are: the problem instance I (made up by a graph G, a travel time matrix $\mathbf{t} \in \mathcal{R}_+^{|V| \times |V|}$, a distance matrix $\mathbf{d} \in \mathcal{R}_+^{|V| \times |V|}$, a demand vector $\mathbf{q} \in \mathcal{R}_+^{|V_C|}$, a delivery robots capacity vector $\mathbf{Q} \in \mathcal{R}_+^{|\Delta|}$, a service time vector $\mathbf{s} \in \mathcal{R}_+^{|V_C|}$, and an average speed $v \in \mathcal{R}_+$), a time limit $T_{\max}$, and the number of neighborhood structures $h_{\max}$ to be used in the VND-like search. We observe that the travel time matrix $\mathbf{t}$ and the distance matrix $\mathbf{d}$ may not necessarily satisfy the triangular inequality.

Let $\mathbf{x}$ be a solution to the ADRRPT, represented by the routes of the ADRs, starting/ending from/at a depot and constituted by a sequence of customer locations and (possibly) some stops of the PTN. The procedure starts by determining an initial solution (Algorithm 1, line 2). Then, the customers set is clustered, by grouping elements based on their spatial characteristics given by $\mathbf{d}$, and an adjacency relationship among clusters according to a dissimilarity measure is computed in such a way that each cluster is adjacent to at least another cluster. This measure is determined on the basis of the minimum distance between two adjacent clusters. The goal of this step is defining an adjacency graph (Algorithm 1, line 4) and identifying solution portions (Algorithm 1, line 5). More details

Algorithm 1 Pseudocode of the coordinated destroy-and-repair metaheuristic

1: **procedure** CoordinatedDestroyAndRepair(I, $T_{\max}$, $h_{\max}$)
2: $\mathbf{x} \leftarrow$ InitialSolution(I)
3: $\mathbf{x}^* \leftarrow \mathbf{x}$ ▷ best found solution
4: $G_a = (V_a, E_a) \leftarrow <$ build the adjacency graph $>$
5: $\mathcal{P} \leftarrow <$ identify solution portions $>$ ▷ $\mathcal{P}$ is the set of solution portions
6: **while** time $\leq T_{\max}$ **do**
7: $\mathbf{x} \leftarrow$ DRP(G_a, $\mathcal{P}$, $\mathbf{x}^*$, $h_{\max}$)
8: **if** $z(\mathbf{x}) < z(\mathbf{x}^*)$ **then** ▷ $z(\mathbf{x})$ denotes the cost of $\mathbf{x}$
9: $\mathbf{x}^* \leftarrow \mathbf{x}$
10: **end if**
11: $(G_a, \mathcal{P}) \leftarrow$ Diversification(I)
12: **end while**
13: **return** $\mathbf{x}^*$
14: **end procedure**

on this step of the algorithm can be found in Section 4.2. This aspect will be key in defining the neighborhoods that are explored with the destroy-and-repair operations throughout the course of the procedure, and will be detailed in Section 4.3. Subsequently, until a time limit is reached, the current solution is updated (Algorithm 1, line 7). If the DRP-based search is propagated through all the solution portions following a VND scheme and there is still time at disposal, a diversification phase is performed trying to explore other parts of the feasibility region (Algorithm 1, line 11). Finally, the best solution is returned. In the following, we detail the different components of our metaheuristic.

4.1. Initial solution construction

To quickly obtain an initial feasible solution $\mathbf{x}$, we first construct routes by aggregating customers that can be serviced directly by an autonomous delivery robot (i.e., the distance from the depot to the customer(s) and back to the depot can be covered with a fully charged robot's battery). To build such set of routes we consider two different strategies: (i) a cheapest-insertion approach (Rosenkrantz et al., 1977); (ii) an approach based on a modification of the Solomon's I1 heuristic (Solomon, 1987). Then, the initial solution is finalized by defining, for each remaining customer, a route that starts from the depot, visits one or more stops of the PTN, services the customer, and returns to the depot via one or more PTN stops.

4.2. Clustering customers and building solution portions

This section provides details on the clustering procedure used to group customers and identify solution portions. The customers are clustered using an unsupervised-learning technique, specifically a straightforward k-means procedure. The value of k is chosen so that the number of customers in each cluster can be easily handled during the repair phase. Let $\mathcal{C} = \{C_1, \dots, C_k\}$ be the resulting set of clusters. Then, an adjacency matrix $\mathcal{A}_C$ between clusters is defined as follows. Let D_i be the minimum distance between cluster C_i and any other cluster in $\mathcal{C}$. The minimum distance between two clusters of $\mathcal{C}$ is the minimum distance on the road graph between any two customers in the clusters. Therefore, D_i represents the distance between C_i and its closest cluster. According to D_i we assume that: (i) each cluster C_i is considered adjacent to its closest cluster, and (ii) a cluster C_j is adjacent to C_i if there exist two customers in C_i and in C_j whose dissimilarity (i.e., their distance on the road graph) is below a given threshold computed as βD_i, where β is a scale parameter. To the adjacency matrix $\mathcal{A}_C$ is associated an undirected graph $G_a(V_a, E_a)$, called *adjacency graph*, in which vertices $i \in V_a$ represent clusters and an edge $(i, j) \in E_a$ exists if vertices (i.e., clusters) $i \in V_a$ and $j \in V_a$ are adjacent according to the predefined dissimilarity measure. Hence, given a solution $\mathbf{x}$ of the ADRRPT, a set $\mathcal{P} = \{P_1, \dots, P_k\}$ of portions of the current solution is determined, where portion P_k is initially obtained by considering all the routes of $\mathbf{x}$ containing customers of cluster C_k. Then, to allow exploring neighborhoods of increasing size, each portion is enlarged with some routes from other portions. These routes visit customers belonging to clusters that are in turn adjacent to cluster C_k. As a result, two portions P_i and P_j, corresponding to clusters C_i and C_j respectively, are adjacent if in the adjacency graph G_a there exists an arc $(i, j) \in E_a$. The enlargement size depends on the value h of the level of the neighborhood hierarchy in the VND. To highlight this dependency, we refer to such a value as n_h in the following, and denote as P_i^h the ith portion enlarged with the routes visiting n_h customers from each cluster adjacent to C_i. Specifically, we select n_h customers from the clusters adjacent to C_i who have the least dissimilarity from any other customer in C_i (see Fig. 4). Fig. 3 reports a graphical representation of the above procedure for an instance with 50 customers, and four clusters. In particular, Fig. 3(a) shows the spatial distribution of the customers, whereas Fig. 3(b) illustrates the four clusters obtained with the k-means procedure. Finally, Figs. 3(c) and 3(d) represent the customers belonging to the solution portion associated with the light-blue cluster, enlarged with one or two customers each from the red, yellow, and purple clusters (that are all adjacent to it), respectively. As a result of this enlarging mechanism, an important aspect of this procedure is its capability to account for the "border effect" when optimizing the solution. This means that parts of the solution that are close to the current portion boundaries can be further improved locally.

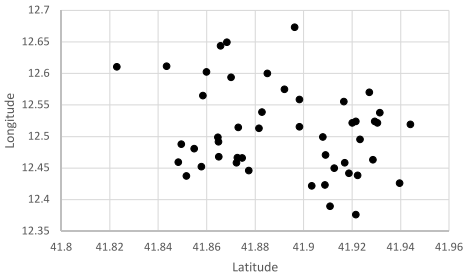

(a) Spatial distribution of the customers

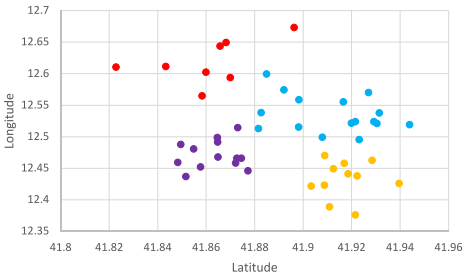

(b) Clusters obtained with the k-means procedure

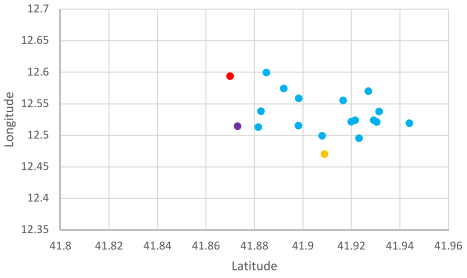

(c) Customers belonging to the solution portion associated with the light-blue cluster when $n_h = 1$

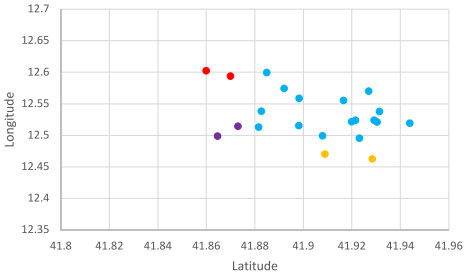

(d) Customers belonging to the solution portion associated with the light-blue cluster when $n_h = 2$

Fig. 3. Obtaining solution portions for a sample instance.

4.3. Destroy-and-repair propagation

In many metaheuristics based on the destroy-and-repair paradigm, repair operators are typically applied to portions of the current solution chosen at random during the destroy phase (Pisinger and Ropke, 2010). In contrast, in this work, our main algorithmic contribution is the definition of the DRP mechanism that exploits the spatial structure of the problem and guides the identification of the parts of the solution to destroy. The methods generally used in the destroy phase typically incorporate elements of randomness when choosing the different parts of the solution to destroy each time the method is called. The neighborhood of a given solution is then defined as the set of solutions that can be reached by first applying the destroy method and then the repair method. The crucial decision to face when implementing the destroy method is the *degree of destruction*. If the destruction is limited to a small fraction of the solution, then the local search heuristic could struggle to explore the search space, as the impact of a large neighborhood is lost. If, however, the destruction involves a significant part, then the heuristic almost degrades to repeated re-optimization. This can be time-consuming or result in poor-quality solutions, depending on how the partial solution is repaired. Spending a lot of time repairing the current solution to optimality can lead to potentially high quality solutions in a few iterations, while it may not be attractive from a diversification point of view, since it incurs the risk of producing identical cost solutions that do not allow escaping from local optima. On the basis of these general observations, the destroy and repair strategies implemented in our metaheuristic are customized to the particular problem and take into consideration its features. First, the destroy process involves selecting a portion of the current solution to remove customers visited on routes that are close each other and which use the same or similar PTN scheduled lines. Second, the repair phase is carried out heuristically by exploiting the possibility of using PTN stops to re-insert a customer into a route at the lowest cost.

Algorithm 2 reports a schematic description of the DRP procedure. Given the adjacency graph G_a, the solution portions $\mathcal{P}$, the best solution $\mathbf{x}^*$, and the value of $h_{\max}$, we maintain a list L of portions to explore, which is initialized with a seed portion P_i randomly chosen in $\mathcal{P}$ (Algorithm 2, lines 3–4), and is visited according to a last-in-first-out (LIFO) policy. Subsequently, until list L becomes empty, a portion P_i is extracted from the end of L, which is then updated with all the solution portions adjacent to P_i and not already present in L (Algorithm 2, lines 6–7). Then, a classical destroy-and-repair operation is performed (Algorithm 2, line 8), in which the destroy part consists in removing from the solution all the routes belonging to portion P_i^h, whereas the repair is performed by re-inserting into the solution each customer of the "destroyed" routes as the result of the best alternative among: (i) inserting the customer into an existing route at the cheapest-insertion cost; (ii) creating (if feasible) a new direct route starting/ending from/at the depot and visiting the customer; (iii) creating a new route starting/ending from/at the depot and visiting the customer via one or more stops of the PTN. If the "repaired" solution improves over the best-found solution, $\mathbf{x}^*$ is updated (Algorithm 2, line 10).

Algorithm 2 Pseudocode of the DRP procedure

1: **procedure** DRP(G_a, $\mathcal{P}$, $\mathbf{x}^*$, $h_{\max}$)
2: $h \leftarrow 1$ ▷ set to 1 the level of the neighborhoods hierarchy
3: $P_i \leftarrow <$ Extract a seed portion from $\mathcal{P}$ $>$ ▷ randomly select a portion from $\mathcal{P}$
4: $L \leftarrow \{P_i\}$ ▷ L is a LIFO list
5: **while** $L \neq \emptyset$ **do**
6: $P_i \leftarrow$ last(L) ▷ pop an element from the end of L
7: $L \leftarrow L \cup \{P_j \in \mathcal{P} \mid \exists (i,j) \in E_a \ \&\& \ P_j \notin L\}$ ▷ add to L all the portions adjacent to p
8: $\mathbf{x} \leftarrow$ DestroyAndRepair($\mathbf{x}^*$, P_i^h)
9: **if** $z(\mathbf{x}) \leq z(\mathbf{x}^*)$ **then**
10: $\mathbf{x}^* \leftarrow \mathbf{x}$
11: **else**
12: $h \leftarrow h + 1$ ▷ increase the neighborhood size
13: **while** $h \leq h_{\max}$ **do**
14: $\mathbf{x} \leftarrow$ DestroyAndRepair($\mathbf{x}^*$, P_i^h)
15: **if** $z(\mathbf{x}) \leq z(\mathbf{x}^*)$ **then**
16: $\mathbf{x}^* \leftarrow \mathbf{x}$
17: $h \leftarrow 1$
18: **break**
19: **else**
20: $h \leftarrow h + 1$
21: **end if**
22: **end while**
23: **end if**
24: **end while**
25: **return** $\mathbf{x}^*$
26: **end procedure**

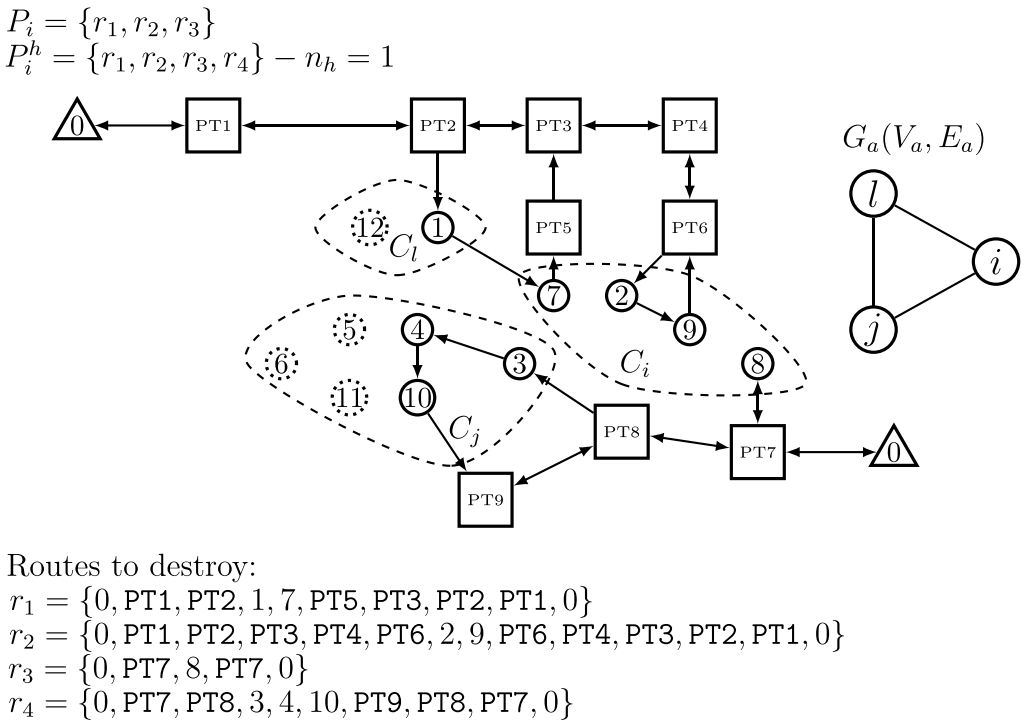

Fig. 4. Example of application of the destroy operator starting from a given portion P_i.

Otherwise, h is iteratively increased by 1, and the destroy-and-repair operation is repeated with the new neighborhood size, until either we obtain an improving solution, or the value $h_{\max}$ is reached, in a classical VND fashion (Algorithm 2, lines 12–22). Finally, the best solution found at the end of this propagation phase is returned (Algorithm 2, line 25).

To provide a practical example of the destroy and repair phases, Fig. 4 depicts a portion made up of routes r_1, r_2 and r_3 for the customers in cluster C_i. This portion is enlarged to include route r_4 visiting customer 3 from the cluster C_j adjacent to C_i. The routes to destroy are shown in bold. Here, for each route, the PTN stops are displayed as square boxes with the stop number preceded by

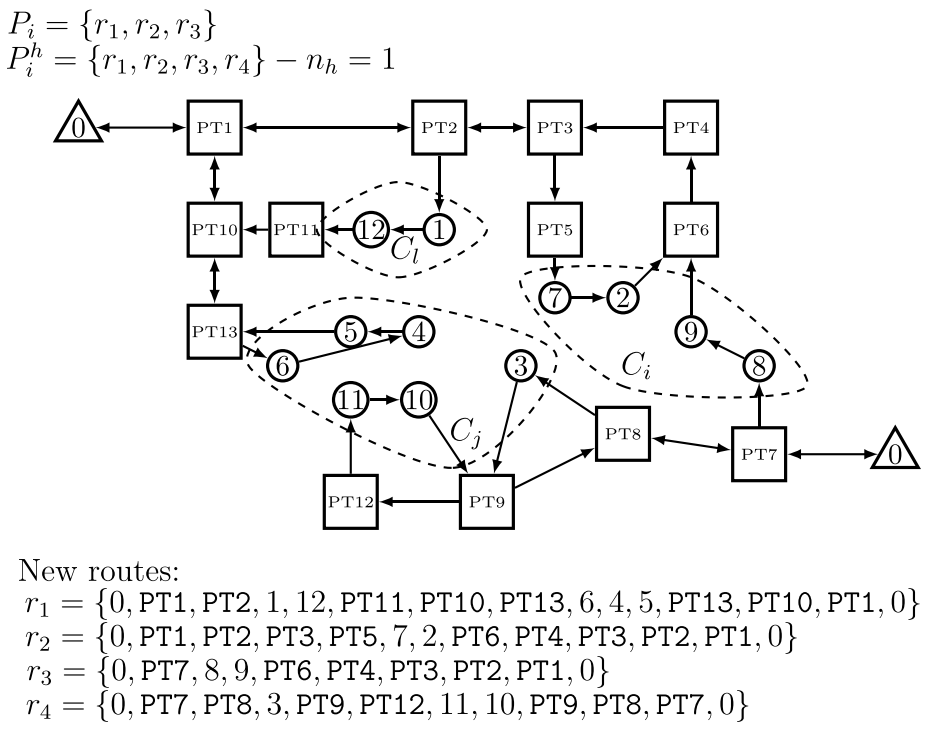

Fig. 5. Example of application of the repair operator.

the prefix "PT". Then, Fig. 5 illustrates the result of the repair step with the updated routes obtained by incorporating the customers removed from the previously identified routes in Fig. 4.

4.4. Diversification

If, at the end of the DRP phase, there is still time at disposal, a diversification phase is performed to favor the exploration of new regions in the solution space. In particular, the diversification step consists in perturbing the distance d_{ij} associated with each arc $(i, j) \in A$. The perturbed value $\overline{d}_{ij}$ is randomly chosen as either $d_{ij} - \gamma d_{ij}$ or $d_{ij} + \gamma d_{ij}$, where $\gamma \in [0, 1]$ is a parameter used to control the perturbation. Then, by considering the perturbed distance matrix $\overline{\mathbf{d}}$, we determine a new adjacency graph G_a and a new set of solution portions $\mathcal{P}$ using the same procedure described in Section 4.2.

5. Computational study

In this section we illustrate the results of the computational study we have performed to assess the effectiveness of our approach. All the algorithms have been coded in Java, and the experiments have been run on a computer with an Intel Core i7 processor clocked at 3.1 GHz with 16 GB of RAM. In the following, we first describe the instances used to test the methodology, and then we present and discuss the results of our experimentation. Finally, we derive some managerial insights by performing an analysis of potential cost and environmental benefits that could be achieved by using the proposed delivery infrastructure, compared to traditional delivery alternatives.

5.1. Instance generation

We observe that the datasets in the literature do not correspond to the problem we are facing, as already pointed out in Section 2. For this reason, we have generated new test instances built from a real pedestrian network and based on a real public transport system, using ADR characteristics in line with those available in recent experiments conducted by Aramex and FedEx. More precisely, to evaluate our approach, we have designed instances resembling drugs distribution to pharmacies in the urban area of Rome (Italy). Real spatial data of customers and stops of the PTN have been extracted from OpenStreetMap (www.openstreetmap.org). The delivery locations are extracted from a set of 751 pharmacies while the PTN stations are 75 stops of the Rome metro system. Finally, we considered a single depot from which we assume that all the ADRs start their routes. Using this data, we have randomly generated 10 different datasets, with 10 instances each, characterized by $|V_P| = 21$ (20 PTN stops and 1 depot), $|V_C| \in \{100, 200, 300, 400, 500\}$, and $Q \in \{4, 20\}$. In the following, the different datasets are labeled as $Q4$–$|V_C|$, or $Q20$–$|V_C|$. Regarding the other features of the

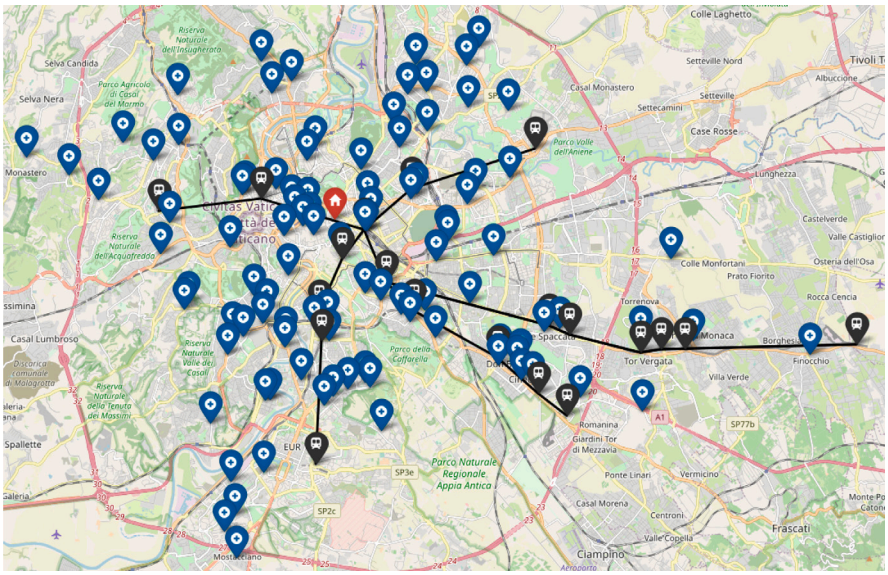

Fig. 6. A sample instance with 100 customers.

instances, we have considered: demand q randomly generated in $\{1, 2, 3, 4, 5\}$, ADRs speed $v = 6$ km/h, service time s randomly generated in $\{2, 3, 4, 5\}$, and maximum distance covered by an ADR with a full battery equal to 16 km. Fig. 6 shows a graphical representation of a sample instance with 100 customers, in which the red pointer represents the depot, the blue pointers represent the pharmacies, the black pointers represent the PTN stops, and the black lines represent direct connections between pairs of PTN stops.

5.2. Parameters settings and benchmark heuristics

To assess the impact of the DRP operator on the solution quality, we compare different strategies under different settings. Specifically, we consider two procedures to obtain an initial solution, namely the cheapest-insertion (CI) heuristic and a heuristic based on a modification of Solomon's I1 insertion (SI) heuristic (see Section 4.1). Moreover, regarding the repair phase, we use two approaches: a single-start (SR) repair heuristic (as described in Section 4.3), and a multi-start repair (MR) heuristic, in which the repair operator is applied m times ($m = 50$, in our tests) by randomly changing the order in which customers are re-inserted into the solution. Overall, the four settings we test are:

- CI–SR: cheapest-insertion-based initial solution and single-start repair;
- SI–SR: Solomon-based initial solution and single-start repair;
- CI–MR: cheapest-insertion-based initial solution and multi-start repair;
- SI–MR: Solomon-based initial solution and multi-start repair.

The quality of the solutions generated by the DRP mechanism is first assessed in comparison with a similar metaheuristic scheme that follows a classic destroy-and-repair approach, in which, at each iteration, we destroy the routes involving μ customers, chosen randomly (random destroy-and-repair, RDR in the following). However, in order to provide a fair comparison, customers are not completely randomly chosen, but, after randomly identifying a seed customers, the remaining $\mu - 1$ customers are selected as the closest to the seed. In our experiments, $\mu = |V_C|/k$. Then, in Section 5.3.1 the DRP solutions are compared with the best lower bound provided by formulation (F-ADRRPT) on a set of instances of reduced size.

The other parameters used for the computational experiments are:

- time limit $T_{\max} = 300$ seconds for the tests involving SR, and $T_{\max} = 1200$ seconds for the tests with MR;
- $h_{\max} = 3$ with $n_1 = 1$, $n_2 = 2$, and $n_3 = 3$;
- number of clusters $k = 10, 20, 30, 40, 50$ when $|V_C| = 100, 200, 300, 400, 500$, respectively;
- scale parameter used for measuring adjacency $\beta = 1.5$;
- diversification parameter $\gamma = 0.1$.

5.3. Analysis of the results

The performances of our approach compared to RDR are assessed by using two indicators: the average percentage deviation of the total travel time of DRP compared to RDR (denoted as DEV_z), and the average percentage deviation of the number of routes in

Table 2
Aggregated results for the datasets $Q4$–100, $Q4$–200, $Q4$–300, $Q4$–400 and $Q4$–500 for the CI–MR, CI–SR, SI–MR, and SI–SR settings.

Dataset	z_I	R_I	z_{DRP}	R_{DRP}	Diversif.	DRP iter.	z_{RDR}	R_{RDR}	RDR iter.	DEV_z	DEV_R
CI–MR											
$Q4$–100	7045.70	67.10	6396.40	66.40	70.60	2065.10	6395.60	66.30	2035.90	0.01%	0.16%
$Q4$–200	13 120.10	131.70	11 772.10	130.00	21.10	1150.10	11 786.30	130.20	1138.30	−0.12%	−0.15%
$Q4$–300	20 156.60	195.90	18 029.90	193.20	9.00	639.40	18 010.50	193.60	643.50	0.11%	−0.21%
$Q4$–400	26 087.80	255.40	23 316.90	253.60	5.90	502.00	23 279.30	253.30	520.60	0.16%	0.12%
$Q4$–500	33 062.10	326.30	29 754.90	323.50	4.30	392.60	29 854.50	322.90	399.30	−0.34%	0.18%
AVG.	19 894.46	195.28	17 854.04	193.34	22.18	949.84	17 865.24	193.26	947.52	−0.03%	0.02%
CI–SR											
$Q4$–100	7045.70	67.10	6654.30	65.80	746.70	22 093.70	6698.30	66.00	21 795.10	−0.65%	−0.29%
$Q4$–200	13 120.10	131.70	12 283.50	129.80	211.90	12 635.00	12 410.00	129.60	12 496.20	−1.01%	0.15%
$Q4$–300	20 156.60	195.90	18 752.10	193.60	81.60	7206.3	18 812.70	193.70	7256.50	−0.34%	−0.05%
$Q4$–400	26 087.80	255.40	24 305.20	253.30	45.00	5223.30	24 391.50	253.70	5250.70	−0.37%	−0.16%
$Q4$–500	33 062.10	326.30	30 769.80	323.60	29.10	4114.50	30 992.80	323.20	4104.40	−0.72%	0.12%
AVG.	19 894.46	195.28	18 552.98	193.22	222.86	10 254.56	18 661.06	193.24	10 180.58	−0.62%	−0.05%
SI–MR											
$Q4$–100	8284.20	76.30	6393.30	66.30	61.50	1788.90	6393.70	66.50	1785.80	0.00%	−0.31%
$Q4$–200	15 934.40	153.00	11 770.80	130.00	19.30	1041.80	11 776.80	130.20	1042.70	−0.06%	−0.16%
$Q4$–300	24 478.10	228.30	18 011.30	193.70	9.70	697.70	18 005.70	193.70	706.00	0.03%	0.00%
$Q4$–400	31 821.70	300.30	23 262.70	253.00	5.90	485.40	23 269.90	253.40	500.00	−0.03%	−0.16%
$Q4$–500	40 287.70	379.30	29 800.00	323.40	4.00	340.90	29 882.40	323.30	355.40	−0.28%	0.03%
AVG.	24 161.22	227.44	17 847.62	193.28	20.08	870.94	17 865.70	193.42	877.98	−0.07%	−0.12%
SI–SR											
$Q4$–100	8284.20	76.30	6594.70	66.10	746.90	22 353.30	6634.50	66.00	21 911.70	−0.61%	0.17%
$Q4$–200	15 934.40	153.00	12 168.20	129.90	208.10	12 374.10	12 256.40	130.00	12 241.20	−0.72%	−0.08%
$Q4$–300	24 478.10	228.30	18 569.90	193.80	91.00	8025.80	18 630.90	193.70	8108.10	−0.32%	0.06%
$Q4$–400	31 821.70	300.30	24 047.00	253.40	45.90	5275.20	24 093.30	253.40	5316.50	−0.20%	0.00%
$Q4$–500	40 287.70	379.30	30 549.50	324.00	30.80	4317.80	30 726.30	323.70	4363.60	−0.57%	0.09%
AVG.	24 161.22	227.44	18 385.86	193.44	224.54	10 469.24	18 468.28	193.36	10 388.22	−0.48%	0.05%

the DRP solution, compared to those of RDR (denoted as DEV_R). The results of this comparison are reported in Tables 2 and 3, which show the average results obtained by the four settings identified in Section 5.2, with $Q = 4$ and $Q = 20$, respectively (the detailed results for all the instances of the various datasets are reported in the Appendix). The tables are organized as follows. Column 'Dataset' indicates the dataset under consideration, columns 'z_I', 'z_{DRP}', and 'z_{RDR}' report the objective function value (i.e., the total travel time) of the initial solution, the best objective function value of DRP, and the best objective function value of RDR, respectively. Columns 'R_I', 'R_{DRP}' and 'R_{RDR}' show the number of routes in the initial solution, and those in the best DRP and RDR solutions, respectively. Column 'Diversif.' reports the number of diversification steps by the DRP algorithm. Columns 'DRP iter.' and 'RDR iter.' show the number of destroy iterations for the DRP and the RDR approaches, respectively. Finally, the values of the average percentage deviations previously described are computed as $DEV_z = (z_{DRP} - z_{RDR})/z_{RDR}$, and $DEV_R = (R_{DRP} - R_{RDR})/R_{RDR}$.

The results reported in Tables 2 and 3 show the effectiveness of the DRP approach. In particular, for the $Q4$ dataset, the values of the average percentage deviation in column DEV_z demonstrate that DRP always improves, on the average, the solution obtained by RDR. Overall, these improvements range between −0.03% and −0.62%. In the disaggregated results reported in the Appendix (see Tables A.10, A.11, A.12, A.13), the maximum improvement reaches −3.54%. Regarding DEV_R, the value ranges between −0.12% and 0.05%. The advantage of DRP over RDR becomes more evident for the $Q20$ dataset. Indeed, Table 3 shows that the larger average percentage deviation in column DEV_z reaches the value of −2.61%. Again, in the disaggregated results reported in the Appendix (Tables A.14 to A.17), the maximum improvement reaches −7.54%. With respect to the number of ADRs used, the values in column DEV_R range between −1.66% and −0.07%. These results prove that the tailored propagation mechanism of the DRP operator allows to perform an in-depth exploration of the feasible region of the problem. In general, DRP outperforms RDR under all settings (CI–MR, CI–SR, SI–MR, and SI–SR). It is worth noting that the DRP mechanism performs better with $Q20$ than with $Q4$, despite the fact that an ADR can execute more deliveries in the former case and the efficiency of the ADR in making deliveries could decrease as a consequence. This is because we observed that when the capacity of the ADRs is small, their routes on the road networks would frequently consist of only one or two deliveries that are close together. Even if there are other delivery locations in the same area that could be served by the same ADR, it would not be possible if the ADR capacity is insufficient. For the instances we designed, when $Q = 4$, a greater number of routes are necessary to serve all customer delivery locations in the same area compared to the case when $Q = 20$. This is evident from the average number of routes (column R_{DRP} in Table 2), which is equal to 193.44, compared to the corresponding value in Table 3, which is equal to 47.52. Thus, the ADRs would require more time to serve all customer delivery locations with a capacity of $Q = 4$ compared to the scenario where they can deliver more packages, i.e., $Q = 20$.

In the following, we perform a statistical analysis aiming to evaluate the different settings for the DRP approach. Figs. 7 and 8 show the statistics computed on the values of DEV_z and DEV_R for the $Q4$ dataset with all the four settings, whereas Figs. 9 and 10 report the same statistics for the $Q20$ dataset. In particular, Fig. 7 highlights that the single-start repair strategy (yellow and orange

Table 3
Aggregated results for the datasets $Q20$–100, $Q20$–200, $Q20$–300, $Q20$–400 and $Q20$–500 for the CI–MR, CI–SR, SI–MR, and SI–SR settings.

Dataset	z_I	R_I	z_{DRP}	R_{DRP}	Diversif.	DRP iter.	z_{RDR}	R_{RDR}	RDR iter.	DEV_z	DEV_R
CI–MR											
$Q20$–100	4151.20	26.50	3130.00	20.60	68.30	1985.70	3117.20	20.40	1858.10	0.40%	1.07%
$Q20$–200	6667.40	42.70	4622.40	32.00	22.50	1221.90	4665.30	32.10	1149.50	−0.90	−0.86%
$Q20$–300	9675.40	60.40	6773.30	46.60	9.60	704.40	6810.80	46.50	695.40	−0.55%	0.23%
$Q20$–400	12 068.70	74.60	8487.00	57.60	4.50	373.80	8550.50	57.90	374.20	−0.73%	−0.51%
$Q20$–500	14 313.30	88.60	10 654.20	71.90	3.00	265.10	10 578.60	72.10	282.30	0.75%	−0.26%
AVG.	9375.20	58.56	6733.38	45.74	21.58	910.18	6744.48	45.84	871.60	−0.21%	−0.07%
CI–SR											
$Q20$–100	4151.20	26.50	3397.90	21.70	883.00	26 436.70	3425.30	22.00	25 003.60	−0.68%	−1.25%
$Q20$–200	6667.40	42.70	5125.80	34.30	180.50	10 725.50	5278.60	34.70	10 508.20	−2.91%	−1.13%
$Q20$–300	9675.4	60.4	7312.3	48.1	82.6	7276.3	7604.9	49.4	7070.5	−3.84%	−2.59%
$Q20$–400	12 068.70	74.60	8931.10	59.20	49.10	5688.00	9225.40	60.40	5537.10	−3.20%	−2.00%
$Q20$–500	14 313.30	88.60	10 950.90	72.70	25.90	3649.70	11 223.50	73.70	3605.00	−2.41%	−1.34%
AVG.	9375.20	58.56	7143.60	47.20	244.22	10 755.24	7351.54	48.04	10 344.88	−2.61%	−1.66%
SI–MR											
$Q20$–100	5682.90	45.40	3125.20	20.60	80.30	2339.00	3111.20	20.50	2239.60	0.47%	0.53%
$Q20$–200	9869.80	84.50	4630.60	32.20	22.20	1181.00	4656.30	32.40	1148.70	−0.55%	−0.61%
$Q20$–300	15 423.90	127.00	6767.10	46.10	9.10	639.80	6790.20	46.20	631.60	−0.33%	−0.18%
$Q20$–400	19 525.40	163.90	8528.20	58.40	5.10	400.70	8558.20	58.40	404.50	−0.35%	0.02%
$Q20$–500	24 158.30	203.10	10 541.30	71.40	3.00	262.30	10 649.00	71.80	274.90	−1.00%	−0.54%
AVG.	14 932.06	124.78	6718.48	45.74	23.94	964.56	6752.98	45.86	939.86	−0.35%	−0.16%
SI–SR											
$Q20$–100	5682.90	45.40	3355.90	22.00	902.30	27 004.20	3437.80	22.20	25 453.20	−2.34%	−0.62%
$Q20$–200	9869.80	84.50	5062.50	33.90	237.00	14 091.00	5254.40	34.40	13 221.60	−3.60%	−1.41%
$Q20$–300	15 423.90	127.00	7337.00	48.70	94.20	8273.30	7525.40	49.30	8147.40	−2.46%	−1.17%
$Q20$–400	19 525.40	163.90	8935.40	59.70	48.00	5529.70	9106.10	60.10	5460.90	−1.88%	−0.66%
$Q20$–500	24 158.30	203.10	10 949.60	73.30	25.70	3598.50	11 087.80	73.60	3605.40	−1.23%	−0.38%
AVG.	14 932.06	124.78	7128.08	47.52	261.44	11 699.34	7282.30	47.92	11 177.70	−2.30%	−0.85%

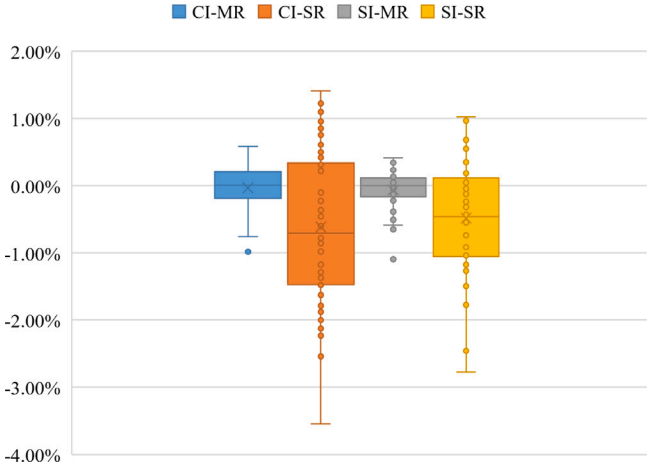

Fig. 7. Boxplots of DEV_z for the CI–MR, CI–SR, SI–MR, and SI–SR on the $Q4$ instances.

boxplots) is significantly better than the multi-start strategy (gray and blue boxplots). The box medians show a high percentage of improved solutions provided by DRP compared with RDR, when the CI–SR and SI–SR settings are used, even if such settings are characterized by a higher dispersion. Regarding the number of routes, Fig. 8 shows that the single-start setting has a similar behavior as the multi-start one in terms of both average improvement and dispersion.

A similar trend emerges in the case of the $Q20$ dataset. Fig. 9 shows how the single-start repair procedure (yellow and orange boxplots) outperforms the multi-start repair (gray and blue boxplots). The box medians associated with the CI–SR and SI–SR settings indicate a significant cost improvement achieved by DRP, compared with RDR. Overall, the increase in the vehicle capacity does not provide significant differences of the deviation DEV_R when comparing the single-start and the multi-start repair approaches as it emerges from Fig. 10.

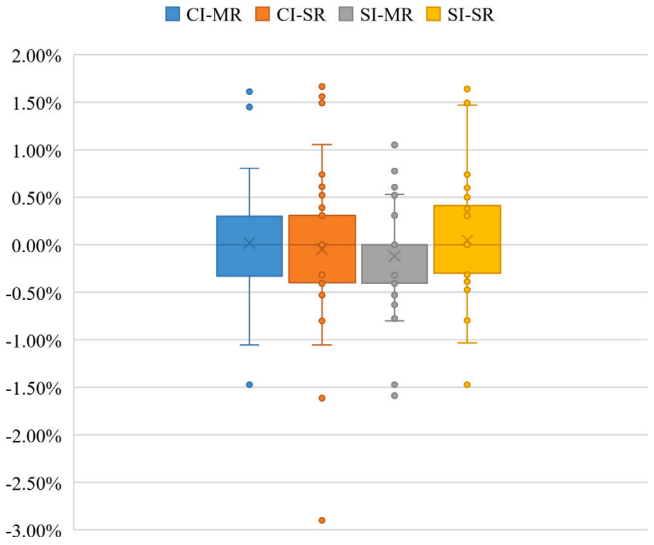

Fig. 8. Boxplots of DEV_R for the CI–MR, CI–SR, SI–MR, and SI–SR settings on the $Q4$ instances.

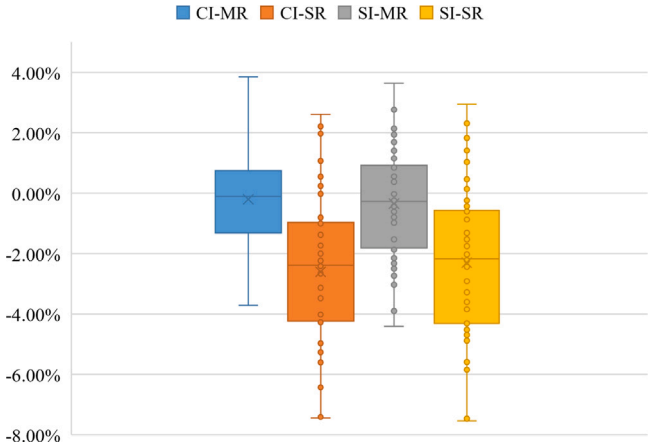

Fig. 9. Boxplots of DEV_z for the CI–MR, CI–SR, SI–MR, and SI–SR settings on the $Q20$ instances.

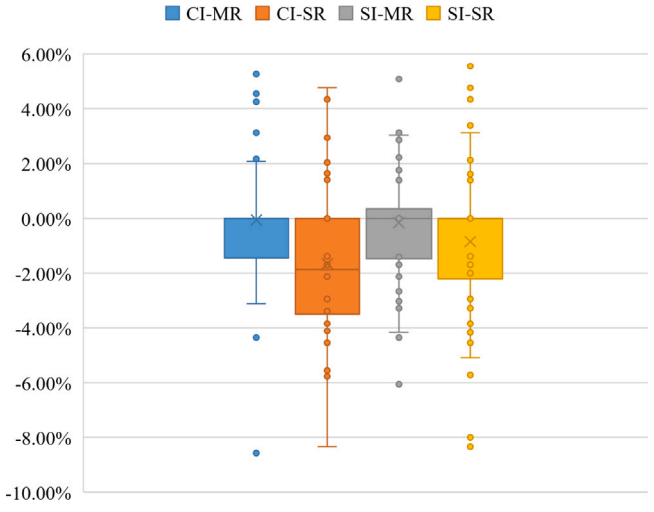

Fig. 10. Boxplots of DEV_R for the CI–MR, CI–SR, SI–MR, and SI–SR settings on the $Q20$ instances.

Table 4
Effectiveness of the heuristic compared to the proposed benchmark.

	CI–MR Q4	CI–SR Q4	SI–MR Q4	SI–SR Q4	CI–MR Q20	CI–SR Q20	SI–MR Q20	SI–SR Q20
$DEV_z \leq 0$	50%	72%	58%	68%	52%	86%	58%	84%
$DEV_z > 0$	50%	28%	42%	32%	48%	14%	42%	16%
$DEV_R \leq 0$	72%	74%	84%	66%	80%	86%	76%	78%
$DEV_R > 0$	28%	26%	16%	34%	20%	14%	24%	22%

Table 5
Comparison of the results obtained by model (1)–(8) and the DRP approach with $Q = 4$.

Instance	z_I	z_{model}	Opt. gap	z_{DRP}	DEV_z	Gap DRP
50_1	4311.00	4196.00	51.00%	3842.00	−8.44%	46.49%
50_2	4192.00	3824.00	55.09%	3485.00	−8.87%	50.72%
50_3	4098.00	4092.00	66.10%	3497.00	−14.54%	60.34%
50_4	4393.00	4099.00	56.36%	3786.00	−7.64%	52.75%
50_5	3888.00	3857.00	56.24%	3524.00	−8.63%	52.10%
50_6	4018.00	3848.00	51.38%	3664.00	−4.78%	48.94%
50_7	4319.00	4187.00	54.93%	3738.00	−10.72%	49.52%
50_8	4570.00	4430.00	51.47%	3856.00	−12.96%	44.24%
50_9	4183.00	4178.00	51.75%	3614.00	−13.50%	44.22%
50_10	4049.00	3934.00	50.46%	3574.00	−9.15%	45.47%
AVG	4202.10	4064.50	54.48%	3658.00	−9.92%	49.48%

With respect to the number of diversification steps and of DRP iterations, from the comparison between the CI–SR and SI–SR settings emerges that the average value of diversifications is around 225 and 250 for the $Q4$ and the $Q20$ datasets, respectively, whereas the average number of DRP iterations is about 10,300 for the $Q4$ dataset, and 11,000 for the $Q20$ dataset. The same comparison between the CI–MR and SI–MR settings brings out the following average values of the number of diversifications: about 21 for the $Q4$ dataset, and about 22 for the $Q20$ dataset. Moreover, the average number of DRP iterations is about 900 for the $Q4$ dataset and around 920 for the $Q20$ dataset. Although the value of $T_{\max}$ imposed for the settings using the multi-start repair is four times the corresponding value used in the single-start repair settings, CI–MR and SI–MR are overall much time consuming than CI–SR and SI–SR. Indeed, the majority of the execution time of the multi-start repair procedure is used to repair the solutions rather than in identifying promising regions to destroy. Therefore, the single-start repair approach allows to better exploit the DRP mechanism.

Finally, we observe that no clear advantages can be achieved by using the cheapest insertion or the Solomon algorithms to generate the initial solutions. To provide more in-depth insights into the results shown in the boxplots, in Table 4 we report the percentage of instances in which DEV_z and DEV_R attain a value less than or equal to zero or greater than zero, respectively. As previously noted, the single-start method once again demonstrates superior performance. Nonetheless, the extensive insights presented in Table 4 emphasize that the DRP heuristic outperforms the baseline. Indeed, in instances where DEV_z does not provide an improvement, there is a corresponding reduction in the number of vehicles deployed (even limited in the multi-start method). From this perspective, it is clear the impact of the "border-reduction effect": extending the clusters by considering close customers and the propagation mechanism favor a better use of the resources. It is worth pointing out that the use of as few vehicles as possible is certainly an important aspect from a management point of view, as will be detailed in Section 5.4.

5.3.1. Comparison with the solution of (F-ADRRPT)

Here, we aim to assess the quality of the solutions provided by our approach compared to the best solution provided by model (F-ADRRPT) within a given time limit. To this purpose, we have generated 10 additional instances of reduced size. More specifically, we have considered $|V_P| = 11$ (10 PTN stops and one depot), $|V_C| = 50$, and $Q \in \{4, 20\}$. Concerning customer demand, service time, ADR speed and maximum distance, we have used the same values of Section 5.1. The mathematical model has been coded in OPL and solved using IBM ILOG CPLEX 22.1.0 with a time limit of 1800 s. On the other hand, for the DRP mechanism, we have considered the CI–SR setting with the same time limit, $k = 3$ clusters, and all the other parameters as in Section 5.2. The results of the comparisons are reported in Tables 5 and 6, for $Q = 4$ and $Q = 20$, respectively. In such tables, 'z_{model}' and 'Opt. gap' report the objective function value of the best solution obtained by formulation (F-ADRRPT) and the optimality gap as reported by the ILP solver at the end of the time limit, respectively. As well known, for a minimization problem the optimality gap is computed as (upper bound − lower bound)/upper bound. This allows to compute a gap for the objective function value of DRP compared to the same lower bound of the optimization model. Such values are reported under the column 'Gap DRP'. The other column headings have the same meaning as in Tables 2 and 3. In particular, 'DEV_z' is the average percentage deviation of z_{DRP}, compared to z_{model}. In order to provide a fair comparison, as a warm start we have provided to the mathematical model the initial solution obtained with the cheapest-insertion approach.

As the tables show, the solver can never find the optimal solution to model (1)–(8) within the given time limit, with an average optimality gap of about 54% for the case with $Q = 4$ and about 70% when $Q = 20$. Indeed, for four instances out of 10 in Table 6, it is

Table 6
Comparison of the results obtained by model (1)–(8) and the DRP approach with $Q = 20$.

Instance	z_I	z_{model}	Opt. gap	z_{DRP}	DEV_z	Gap DRP
50_1	3301.00	3301.00	67.52%	2444.00	−25.96%	56.14%
50_2	3126.00	3126.00	71.53%	2060.00	−34.10%	56.80%
50_3	2663.00	2646.00	68.03%	1993.00	−24.68%	57.55%
50_4	3152.00	3151.00	65.47%	2171.00	−31.10%	49.88%
50_5	2801.00	2713.00	65.94%	2211.00	−18.50%	58.21%
50_6	3091.00	3091.00	74.09%	1971.00	−36.23%	59.37%
50_7	3041.00	2866.00	74.67%	2142.00	−25.26%	66.12%
50_8	3502.00	3293.00	70.78%	2411.00	−26.78%	60.10%
50_9	3291.00	3253.00	66.50%	2387.00	−26.62%	54.35%
50_10	3083.00	3083.00	76.73%	2044.00	−33.70%	64.90%
AVG.	3105.10	3052.30	70.13%	2183.40	−28.29%	58.34%

Table 7
Technological and cost parameters for the different types of vehicles.

Parameter	ADR-PT	DV	EV
Average speed (km/h)	6	30	30
Emissions (kg of CO_2/km)	0.001	0.200	0.010
Energy consumption (kWh/km)	0.0247	–	0.215
Fuel cost (€/km)	–	0.15	–
Unit energy cost (€/kWh)	0.30	–	0.30
Vehicle cost (€/day)	5	30	50
Staff cost per vehicle (€/day)	20	200	200

not able to find a solution with an objective function value better than z_I. On the other hand, the value of z_{DRP} always outperforms that of z_{model}, with an average deviation of about −10% when the ADR capacity is the lowest, and about −28% with $Q = 20$. Finally, concerning the gap of z_{DRP} compared to the lower bound obtained by the solver, we observe lower gaps in Table 5, with values ranging between about 44% and 60%, with an average value of about 49%. When the delivery robots capacity increases, the gaps increase to achieve an average value of about 58%, with minimum and maximum values of about 49% and about 66%, respectively.

5.4. Managerial insights

In this section, we derive some insights related to the potential cost and environmental advantages of using ADRs combined with PT, compared to delivery by means of traditional vehicles, being either diesel-powered or electric-powered vans. To this purpose, we run the DRP approach in which customers requests must be serviced by: (i) a fleet of ADRs in combination with PT vehicles (ADR-PT in the following), as reported in Section 5.3; (ii) a fleet of traditional diesel-fueled vans (DV in the following); (iii) a fleet of electric-powered vans (EV in the following). In the two latter cases, we neglect the presence of PT vehicles.

The three alternatives are compared under the CI–SR setting, with the same input parameters of Section 5.3, whereas the technological and cost parameters for the different types of vehicles are reported in Table 7. Following Raghunatha et al. (2023) (who make a comparison between air drones and traditional delivery vehicles), we have considered the Ford Transit 310 L3 H2 2.0L ECOBLUE,[1] for DVs, and the Volkswagen E-crafter,[2] for EVs, as reference vans. Regarding a reference autonomous delivery robot, we have considered a vehicle with characteristics similar to the robot by Starship,[3] which is also considered in a study by Figliozzi (2020). Concerning the daily cost of vehicles, we have considered a life cycle of five years with 200 days of usage per year, and a buying cost of 4000 € for autonomous delivery robots, 30,000 € for DV, and 50,000 € for EV. The staff cost per vehicle (the cost of the driver for DV and EV, and the cost of the worker in charge of loading the parcels on the robots for ADR-PT) has been obtained by assuming an annual wage of 40,000 € and 200 working days per year. Moreover, the value for ADR-PT has been computed by assuming that a worker controls 10 ADRs each day. With respect to the emissions for EV and ADR-PT, we have obtained the values reported in Table 7 by multiplying the emissions per unit of energy expressed in kg of CO_2/kWh and the energy consumption expressed in kWh/km. The former value is 0.047 (see Raghunatha et al., 2023) for both types of vehicles, whereas the latter value is 0.0247 (see Figliozzi, 2020) and 0.215 (see Raghunatha et al., 2023) for ADR-PT and EV, respectively. Finally, the fuel cost for DV has been computed by considering a cost of 1.80 €/l of diesel fuel and an average consumption of 8.2 l/100 km (assuming mixed driving).

The results of our managerial analysis are shown in Tables 8 and 9. In particular, Table 8 reports the number of vehicles needed to service all the customers (N_V), as well as the total distance traveled by such vehicles (TD). Not surprisingly, the number of

[1] https://corporate.ford.com/articles/history/the-ford-transit.html
[2] https://www.volkswagen-vans.co.uk/en/about-us/van-life/ecrafter.html
[3] https://www.starship.xyz

Table 8
Number of vehicles needed and total traveled distance (in km) for the different types of vehicles.

Size	DV and EV		ADR-PT	
	N_V	TD	N_V	TD
100	6.70	328.58	21.70	303.87
200	11.60	551.39	34.30	461.91
300	16.40	780.16	48.10	666.45
400	21.20	1,005.60	59.20	820.04
500	25.70	1,242.35	72.70	995.45
AVG	16.32	781.62	47.20	649.54

Table 9
Cost (in €) and emission (in kg of CO_2) analysis for the different types of vehicles.

Size	DV		EV		ADR-PT		Comparison ADR-PT – DV		Comparison ADR-PT – EV	
	Cost	Emiss.	Cost	Emiss.	Cost	Emiss.	DEV_C	DEV_E	DEV_C	DEV_E
100	1,589.50	65.72	1,696.19	3.32	554.75	0.35	−65.01%	−99.46%	−67.21%	−89.35%
200	2,749.39	110.28	2,935.56	5.57	860.92	0.54	−68.64%	−99.51%	−70.63%	−90.35%
300	3,887.15	156.03	4,150.32	7.88	1,219.94	0.77	−68.57%	−99.50%	−70.57%	−90.16%
400	5,024.43	201.12	5,364.86	10.16	1,503.58	0.95	−70.05%	−99.53%	−71.95%	−90.60%
500	6,094.37	248.47	6,505.13	12.55	1,834.88	1.16	−69.88%	−99.53%	−71.78%	−90.78%
AVG	3,868.97	56.32	4,130.41	7.90	1,194.81	0.75	−68.43%	−99.51%	−70.43%	−90.25%

vehicles needed when using ADRs is always greater that DV and EV, given their lower range and limited capacity. On the other hand, the possibility to use the PTN allows ADRs to travel a smaller distance than DV and EV. These results are then used in Table 9 to derive some managerial insights with respect to costs and emissions of the different types of vehicles. Here, the cost is obtained as the sum of: (i) N_V (from Table 8) multiplied by the sum of vehicle cost and staff cost (from Table 7); TD (from Table 8) multiplied by the fuel cost per km for DV or the energy cost per km for ADR-PT and EV, obtained as the product of the energy consumption and the unit energy cost per kWh (Table 7). Regarding the emissions, they are computed as the product of TD and the value in kg of CO_2/km from Table 7. The percentage deviations of costs and emissions (denoted as DEV_C and DEV_E, respectively) related to using ADR-PT versus DV and EV show that using autonomous delivery robots combined with the PTN can provide huge benefits in terms of both indicators. In particular, the average percentage cost deviation is about 68.5% when compared to DV, and about 70.5% when compared to EV. The advantage becomes more evident as the number of customers grows. The benefit is even more important in terms of emissions. More specifically, the average deviation of ADR-PT versus DV is about 99.5%, with this value slightly decreasing to about 90% when comparing to EV. In this case, we do not observe significant changes as the size of the instances grows.

6. Conclusions

Autonomous delivery robots can be combined with the public transportation system to obtain a more sustainable last-mile distribution, especially suited for densely populated urban areas. In this paper, we have considered the problem of determining the best routes to be traveled by ADRs, including synchronization with the PT lines. In order to tackle the problem, we introduced a tailored destroy-and-repair mechanism, able to take advantage from the geographical structure of the PTN. This operator implements a sort of propagation during the destroy iterations that produces a faster improvement of the solution during the neighborhoods exploration. The proposed mechanism was then embedded into a neighborhood search algorithm and compared with a similar metaheuristic scheme based on a traditional random destroy approach. Results on instances with up to 500 requests, inspired by a real-world distribution problem, showed that the proposed approach can provide solution improvements up to about 7.5%, and a maximum reduction of the number of ADRs needed of about 8.5%. From a managerial point of view, our experiments have shown that using the proposed infrastructure of autonomous delivery robots combined with the public transportation network can provide huge benefits in terms of both costs and emissions reduction. Future studies might extend this approach to different operational constraints, such as time windows constraints as well as consider different objective functions. Additionally, potential sources of uncertainty, including travel times or the residual battery charge, could be considered and assessed in future work.

CRediT authorship contribution statement

Annarita De Maio: Writing – review & editing, Writing – original draft, Validation, Investigation, Data curation, Conceptualization. **Gianpaolo Ghiani:** Writing – review & editing, Writing – original draft, Validation, Supervision, Methodology, Investigation, Funding acquisition, Data curation, Conceptualization. **Demetrio Laganà:** Writing – review & editing, Writing – original draft, Validation, Investigation, Data curation, Conceptualization. **Emanuele Manni:** Writing – review & editing, Writing – original draft, Validation, Supervision, Software, Methodology, Investigation, Data curation, Conceptualization.

Acknowledgments

The authors would like to thank the associate editor and the anonymous reviewers for the constructive and thorough comments, which significantly contributed to the improvement of the manuscript during the revision process. The work of Gianpaolo Ghiani and Emanuele Manni has been partly supported by the research program "Sustainable Mobility Center" (Centro Nazionale per la Mobilità Sostenibile - CN MOST, Italy), project code CN00000023, Spoke 7. The work of Annarita De Maio has been partly supported by MUR (Italian Minister of University and Research), Italy under the grant H25F21001230004. These supports are gratefully acknowledged.

Appendix. Disaggregated results

Tables A.10, A.11, A.12, and A.13 report the results for the datasets groups *Q*4–100, *Q*4–200, *Q*4–300, *Q*4–400, and *Q*4–500 considering the CI–MR, CI–SR, SI–MR and SI–SR settings, respectively. Tables A.14, A.15, A.16, and A.17 report the results for the datasets *Q*20–100, *Q*20–200, *Q*20–300, *Q*20–400, and *Q*20–500 considering the CI–MR, CI–SR, SI–MR and SI–SR settings, respectively.

Table A.10
Results for the datasets *Q*4–100, *Q*4–200, *Q*4–300, *Q*4–400, and *Q*4–500 for the CI–MR setting.

Dataset	z_I	R_I	z_{DRP}	R_{DRP}	Diversif.	DRP iter.	z_{RDR}	R_{RDR}	RDR iter.	DEV_z	DEV_R
*Q*4–100_1	7452	68	6587	68	74	2186	6587	68	2243	0.00%	0.00%
*Q*4–100_2	6843	69	6191	70	79	2325	6187	70	2286	0.06%	0.00%
*Q*4–100_3	7541	70	6901	68	77	2278	6901	68	2282	0.00%	0.00%
*Q*4–100_4	7131	63	6283	61	57	1654	6299	61	1611	−0.25%	0.00%
*Q*4–100_5	7371	66	6855	67	76	2220	6857	67	2239	−0.03%	0.00%
*Q*4–100_6	7432	69	6674	67	70	2037	6660	68	2012	0.21%	−1.47%
*Q*4–100_7	6891	63	6279	63	76	2216	6277	62	2131	0.03%	1.61%
*Q*4–100_8	7108	69	6551	68	60	1753	6551	68	1730	0.00%	0.00%
*Q*4–100_9	6764	72	6308	70	65	1892	6308	69	1836	0.00%	1.45%
*Q*4–100_10	5924	62	5335	62	72	2090	5329	62	1989	0.11%	0.00%
*Q*4–200_1	13 771	133	12 472	129	24	1327	12 510	129	1324	−0.30%	0.00%
*Q*4–200_2	12 900	129	11 737	128	21	1111	11 759	129	1083	−0.19%	−0.78%
*Q*4–200_3	12 900	131	11 715	130	23	1269	11 711	129	1203	0.03%	0.78%
*Q*4–200_4	13 110	132	11 799	129	18	958	11 762	129	947	0.31%	0.00%
*Q*4–200_5	13 620	137	12 378	136	22	1239	12 434	136	1207	−0.45%	0.00%
*Q*4–200_6	12 967	127	11 259	128	24	1332	11 274	128	1328	−0.13%	0.00%
*Q*4–200_7	12 320	127	11 007	125	19	990	11 041	125	972	−0.31%	0.00%
*Q*4–200_8	13 604	135	12 178	132	23	1291	12 202	132	1301	−0.20%	0.00%
*Q*4–200_9	13 583	137	12 303	136	19	1045	12 322	137	1065	−0.15%	−0.73%
*Q*4–200_10	12 426	129	10 873	127	18	939	10 848	128	953	0.23%	−0.78%
*Q*4–300_1	19 640	191	17 837	189	9	630	17 830	189	645	0.04%	0.00%
*Q*4–300_2	20 274	196	18 222	192	10	716	18 185	193	717	0.20%	−0.52%
*Q*4–300_3	21 447	202	18 596	200	10	696	18 627	200	704	−0.17%	0.00%
*Q*4–300_4	19 725	212	18 102	211	7	518	18 098	210	510	0.02%	0.48%
*Q*4–300_5	19 805	193	17 777	189	8	602	17 764	189	616	0.07%	0.00%
*Q*4–300_6	21 696	192	19 583	191	9	606	19 540	191	609	0.22%	0.00%
*Q*4–300_7	19 970	192	18 217	188	9	668	18 215	189	679	0.01%	−0.53%
*Q*4–300_8	17 982	195	16 170	193	8	546	16 136	192	563	0.21%	0.52%
*Q*4–300_9	21 085	191	18 512	188	9	618	18 405	190	638	0.58%	−1.05%
*Q*4–300_10	19 942	195	17 283	191	11	794	17 305	193	754	−0.13%	−1.04%
*Q*4–400_1	25 643	250	22 724	246	7	579	22 654	247	591	0.31%	−0.40%
*Q*4–400_2	24 060	261	21 099	258	6	454	21 096	259	563	0.01%	−0.39%
*Q*4–400_3	26 826	257	24 045	256	6	455	24 023	254	453	0.09%	0.79%
*Q*4–400_4	26 152	252	23 457	251	6	541	23 350	250	550	0.46%	0.40%
*Q*4–400_5	25 879	254	23 289	250	6	518	23 181	248	535	0.47%	0.81%
*Q*4–400_6	26 100	264	23 695	263	6	551	23 628	263	565	0.28%	0.00%
*Q*4–400_7	26 387	256	23 697	253	6	504	23 639	254	521	0.25%	−0.39%
*Q*4–400_8	28 029	253	24 752	252	6	520	24 674	252	539	0.32%	0.00%
*Q*4–400_9	26 389	258	23 810	256	5	463	23 907	257	462	−0.41%	−0.39%
*Q*4–400_10	25 413	249	22 601	251	5	435	22 641	249	427	−0.18%	0.80%
*Q*4–500_1	32 715	334	29 089	332	4	313	29 235	331	31	−0.50%	0.30%
*Q*4–500_2	31 294	329	28 597	329	4	355	28 606	328	353	−0.03%	0.30%
*Q*4–500_3	31 948	312	28 258	310	5	424	28 354	310	435	−0.34%	0.00%
*Q*4–500_4	35 079	339	31 545	333	4	413	31 664	332	417	−0.38%	0.30%
*Q*4–500_5	34390.	327	31 083	325	4	381	31 094	323	383	−0.04%	0.62%
*Q*4–500_6	32 332	320	28 837	316	4	394	29 057	316	404	−0.76%	0.00%
*Q*4–500_7	33 054	330	30 106	328	4	389	30 258	328	396	−0.50%	0.00%
*Q*4–500_8	34 401	325	31 199	322	4	395	31 154	320	415	0.14%	0.63%
*Q*4–500_9	33 124	322	29 560	319	5	411	29 854	319	424	−0.98%	0.00%
*Q*4–500_10	32 284	325	29 275	321	5	451	29 269	322	455	0.02%	−0.31%
AVG.	19 894.50	195.30	17 854.00	193.30	22.20	949.80	17 865.20	193.30	947.50	−0.03%	0.002%

Table A.11
Results for the datasets *Q*4–100, *Q*4–200, *Q*4–300, *Q*4–400 and *Q*4–500 for the CI–SR setting.

Dataset	z_I	R_I	z_{DRP}	R_{DRP}	Diversif.	DRP iter.	z_{RDR}	R_{RDR}	RDR iter.	DEV_z	DEV_R
*Q*4–100_1	7452	68	6804	68	766	22 935	6943	67	22 971	−2.00%	1.49%
*Q*4–100_2	6843	69	6441	69	800	23 958	6581	69	23 001	−2.13%	0.00%
*Q*4–100_3	7541	70	7126	67	812	24 324	7066	69	24 729	0.85%	−2.90%
*Q*4–100_4	7131	63	6509	61	698	18 196	6560	60	17 578	−0.78%	1.67%
*Q*4–100_5	7371	66	7033	66	849	25 438	7138	66	24 238	−1.47%	0.00%
*Q*4–100_6	7432	69	7113	67	702	21 016	7046	67	21 654	0.95%	0.00%
*Q*4–100_7	6891	63	6476	62	789	23 630	6624	63	22 248	−2.23%	−1.59%
*Q*4–100_8	7108	69	6905	68	630	18 867	6827	68	19 064	1.14%	0.00%
*Q*4–100_9	6764	72	6464	69	718	21 512	6554	69	21 296	−1.37%	0.00%
*Q*4–100_10	5924	62	5672	61	703	21 061	5644	62	21 172	0.50%	−1.61%
*Q*4–200_1	13 771	133	12 990	129	251	14 958	12 849	130	15 357	1.10%	−0.77%
*Q*4–200_2	12 900	129	12 108	129	202	12 043	12 553	127	11 627	−3.54%	1.57%
*Q*4–200_3	12 900	131	12 096	130	237	14 146	12 152	128	13 742	−0.46%	1.56%
*Q*4–200_4	13 110	132	12 351	129	178	10 566	12 673	129	10 209	−2.54%	0.00%
*Q*4–200_5	13 620	137	12 905	136	225	13 412	13 017	135	13 041	−0.86%	0.74%
*Q*4–200_6	12 967	127	11 887	127	241	14 386	12 098	127	14 535	−1.74%	0.00%
*Q*4–200_7	12 320	127	11 526	124	185	11 026	11 387	125	10 991	1.22%	−0.80%
*Q*4–200_8	13 604	135	12 509	132	238	14 208	12 789	132	14 158	−2.19%	0.00%
*Q*4–200_9	13 583	137	13 133	136	187	11 186	13 035	136	11 237	0.75%	0.00%
*Q*4–200_10	12 426	129	11 330	126	175	10 419	11 547	127	10 065	−1.88%	−0.79%
*Q*4–300_1	19 640	191	18 433	188	79	6962	18 376	190	7153	0.31%	−1.05%
*Q*4–300_2	20 274	196	18 801	193	87	7714	19 112	193	7835	−1.63%	0.00%
*Q*4–300_3	21 447	202	19 415	200	89	7832	19 646	201	7632	−1.18%	−0.50%
*Q*4–300_4	19 725	212	18 839	211	66	5843	18 761	211	5690	0.42%	0.00%
*Q*4–300_5	19 805	193	18 290	191	78	6839	18 351	189	7043	−0.33%	1.06%
*Q*4–300_6	21 696	192	20 475	189	76	6702	20 191	190	6934	1.41%	−0.53%
*Q*4–300_7	19 970	192	19 008	191	84	7419	19 028	190	7818	−0.11%	0.53%
*Q*4–300_8	17 982	195	16 716	193	70	6174	16 945	192	6058	−1.35%	0.52%
*Q*4–300_9	21 085	191	19 290	188	77	6816	19 428	189	6523	−0.71%	−0.53%
*Q*4–300_10	19 942	195	18 254	192	110	9762	18 289	192	9879	−0.19%	0.00%
*Q*4–400_1	25 643	250	23 427	246	53	6175	23 806	247	6158	−1.59%	−0.40%
*Q*4–400_2	24 060	261	21 919	258	42	4818	22 129	258	4799	−0.95%	0.00%
*Q*4–400_3	26 826	257	25 372	256	39	4505	25 624	255	4542	−0.98%	0.39%
*Q*4–400_4	26 152	252	24 343	251	48	5558	24 491	251	5471	−0.60%	0.00%
*Q*4–400_5	25 879	254	24 317	249	47	5512	24 373	249	5646	−0.23%	0.00%
*Q*4–400_6	26 100	264	24 715	263	51	5960	24 757	264	5906	−0.17%	−0.38%
*Q*4–400_7	26 387	256	24 509	254	47	5433	24 595	256	5540	−0.35%	−0.78%
*Q*4–400_8	28 029	253	26 034	251	45	5249	25 748	252	5368	1.11%	−0.40%
*Q*4–400_9	26 389	258	24 735	257	40	4687	24 525	257	4789	0.86%	0.00%
*Q*4–400_10	25 413	249	23 681	248	38	4336	23 867	248	4288	−0.78%	0.00%
*Q*4–500_1	32 715	334	29 953	333	24	3235	30 301	333	3236	−1.15%	0.00%
*Q*4–500_2	31 294	329	29 631	330	25	3580	29 843	328	3614	−0.71%	0.61%
*Q*4–500_3	31 948	312	29 515	310	30	4256	29 451	310	4303	0.22%	0.00%
*Q*4–500_4	35 079	339	32 483	333	31	4345	32 602	333	4202	−0.37%	0.00%
*Q*4–500_5	34 390	327	31 790	323	29	4008	32 268	323	3975	−1.48%	0.00%
*Q*4–500_6	32 332	320	30 172	316	29	4159	30 399	317	4069	−0.75%	−0.32%
*Q*4–500_7	33 054	330	31 136	329	29	4135	30 948	327	4309	0.61%	0.61%
*Q*4–500_8	34 401	325	32 071	321	30	4274	32 217	320	4238	−0.45%	0.31%
*Q*4–500_9	33 124	322	30 521	319	31	4400	31 076	320	4303	−1.79%	−0.31%
*Q*4–500_10	32 284	325	30 426	322	33	4753	30 823	321	4795	−1.29%	0.31%
AVG.	19 894.50	195.30	18 553.00	193.20	222.90	10 254.60	18 661.10	193.20	10 180.60	−0.062%	−0.05%

Table A.12
Results for the datasets *Q*4–100, *Q*4–200, *Q*4–300, *Q*4–400, and *Q*4–500 for the SI–MR setting.

Dataset	z_{I}	R_{I}	z_{DRP}	R_{DRP}	Diversif.	DRP iter.	z_{RDR}	R_{RDR}	RDR iter.	DEV_z	DEV_R
*Q*4–100_1	8505	78	6587	68	71	2072	6587	68	2060	0.00%	0.00%
*Q*4–100_2	7828	77	6187	70	72	2102	6187	70	2086	0.00%	0.00%
*Q*4–100_3	9530	83	6901	68	67	1949	6910	68	1898	−0.13%	0.00%
*Q*4–100_4	7964	69	6261	62	48	1387	6281	62	1501	−0.32%	0.00%
*Q*4–100_5	8314	77	6855	67	68	1992	6855	67	1866	0.00%	0.00%
*Q*4–100_6	8800	79	6669	67	55	1603	6657	68	1616	0.18%	−1.47%
*Q*4–100_7	8175	76	6277	62	63	1826	6282	63	1807	−0.08%	−1.59%
*Q*4–100_8	8158	77	6551	68	46	1341	6551	68	1540	0.00%	0.00%
*Q*4–100_9	8275	78	6310	70	60	1736	6301	70	1701	0.14%	0.00%
*Q*4–100_10	7293	69	5335	61	65	1881	5326	61	1783	0.17%	0.00%
*Q*4–200_1	16 139	152	12 468	128	23	1234	12 447	129	1239	0.17%	−0.78%
*Q*4–200_2	15 049	150	11 758	129	19	1001	11 722	130	960	0.31%	−0.77%
*Q*4–200_3	15 824	154	11 707	129	21	1166	11 725	129	1114	−0.15%	0.00%
*Q*4–200_4	16 551	152	11 753	130	16	862	11 765	129	868	−0.10%	0.78%
*Q*4–200_5	16 977	159	12 373	136	20	1105	12 385	136	1144	−0.10%	0.00%
*Q*4–200_6	14 665	149	11 328	128	22	1213	11 302	128	1231	0.23%	0.00%
*Q*4–200_7	15 201	149	11 005	124	17	891	11 057	125	873	−0.47%	−0.80%
*Q*4–200_8	15 886	153	12 173	132	21	1137	12 184	132	1180	−0.09%	0.00%
*Q*4–200_9	16 841	156	12 315	136	18	967	12 315	136	969	0.00%	0.00%
*Q*4–200_10	16 211	156	10 828	128	16	842	10 866	128	849	−0.35%	0.00%
*Q*4–300_1	24 396	221	17 819	188	9	682	17 827	189	713	−0.04%	−0.53%
*Q*4–300_2	24 625	230	18 153	192	11	792	18 141	193	788	0.07%	−0.52%
*Q*4–300_3	24 873	237	18 599	200	10	747	18 663	201	748	−0.34%	−0.50%
*Q*4–300_4	25 047	239	18 081	210	8	567	18 072	210	563	0.05%	0.00%
*Q*4–300_5	23 727	223	17 756	190	10	665	17 751	190	683	0.03%	0.00%
*Q*4–300_6	25 591	222	19 548	192	9	645	19 527	190	675	0.11%	1.05%
*Q*4–300_7	24 883	224	18 253	189	10	731	18 256	190	737	−0.02%	−0.53%
*Q*4–300_8	22 914	229	16 131	193	9	618	16 126	193	634	0.03%	0.00%
*Q*4–300_9	25 096	229	18 422	190	10	696	18 414	189	685	0.04%	0.53%
*Q*4–300_10	23 629	229	17 351	193	11	834	17 280	192	834	0.41%	0.52%
*Q*4–400_1	31 241	295	22 769	245	6	535	22 692	246	570	0.34%	−0.41%
*Q*4–400_2	30 679	309	21 032	258	5	427	21 005	258	457	0.13%	0.00%
*Q*4–400_3	32 284	298	24 048	254	5	433	24 044	255	426	0.02%	−0.39%
*Q*4–400_4	33 245	302	23 405	250	7	520	23 406	251	530	0.00%	−0.40%
*Q*4–400_5	31 333	297	23 261	249	6	524	23 275	249	520	−0.06%	0.00%
*Q*4–400_6	31 333	304	23 631	263	7	558	23 670	263	568	−0.16%	0.00%
*Q*4–400_7	31 911	295	23 548	254	6	502	23 668	254	523	−0.51%	0.00%
*Q*4–400_8	32 825	297	24 716	252	6	492	24 682	252	518	0.14%	0.00%
*Q*4–400_9	32 163	303	23 748	257	6	453	23 801	257	456	−0.22%	0.00%
*Q*4–400_10	31 203	303	22 469	248	5	410	22 456	249	432	0.06%	−0.40%
*Q*4–500_1	40 288	383	29 177	332	4	268	29 500	330	277	−1.09%	0.61%
*Q*4–500_2	38 828	378	28 598	330	4	305	28 785	328	309	−0.65%	0.61%
*Q*4–500_3	39 364	367	28 332	310	4	346	28 383	311	372	−0.18%	−0.32%
*Q*4–500_4	41 534	388	31 518	333	4	361	31 633	333	363	−0.36%	0.00%
*Q*4–500_5	41 481	379	31 137	324	4	331	31 259	323	358	−0.39%	0.31%
*Q*4–500_6	39 690	374	28 894	316	4	346	28 910	318	353	−0.06%	−0.63%
*Q*4–500_7	40 895	385	30 162	328	4	355	30 341	329	361	−0.59%	−0.30%
*Q*4–500_8	39 994	374	31 149	320	4	343	31 101	320	371	0.15%	0.00%
*Q*4–500_9	41 384	387	29 796	318	4	356	29 692	319	381	0.35%	−0.31%
*Q*4–500_10	39 419	378	29 237	323	4	398	29 220	322	409	0.06%	0.31%
AVG.	24 161.2	227.4	17 847.6	193.3	20.1	870.9	17 865.7	193.4	878.0	−0.07%	−0.12%

Table A.13
Results for the datasets $Q4$–100, $Q4$–200, $Q4$–300, $Q4$–400, and $Q4$–500 for the SI–SR setting.

Dataset	z_I	R_I	z_{DRP}	R_{DRP}	Diversif.	DRP iter.	z_{RDR}	R_{RDR}	RDR iter.	DEV_z	DEV_R
$Q4$–100_1	8505	78	6902	67	814	24 378	6899	68	24 491	0.04%	−1.47%
$Q4$–100_2	7828	77	6507	69	807	24 162	6501	70	23 199	0.09%	−1.43%
$Q4$–100_3	9530	83	7024	68	822	24 587	7059	67	24 277	−0.50%	1.49%
$Q4$–100_4	7964	69	6467	61	615	18 418	6470	61	17 698	−0.05%	0.00%
$Q4$–100_5	8314	77	7056	66	844	25 262	7130	66	23 567	−1.04%	0.00%
$Q4$–100_6	8800	79	6900	68	723	21 626	6834	68	22 920	0.97%	0.00%
$Q4$–100_7	8175	76	6390	62	799	23 903	6551	62	22 452	−2.46%	0.00%
$Q4$–100_8	8158	77	6803	69	621	18 583	6881	69	18 602	−1.13%	0.00%
$Q4$–100_9	8275	78	6463	69	708	21 189	6521	68	20 732	−0.89%	1.47%
$Q4$–100_10	7293	69	5435	62	716	21 425	5499	61	21 179	−1.16%	1.64%
$Q4$–200_1	16 139	152	12 933	129	233	13 888	12 964	130	14 709	−0.24%	−0.77%
$Q4$–200_2	15 049	150	12 039	128	202	12 008	12 182	129	11 560	−1.17%	−0.78%
$Q4$–200_3	15 824	154	12 063	129	233	13 847	12 021	130	13 815	0.35%	−0.77%
$Q4$–200_4	16 551	152	12 117	130	175	10 399	12 463	129	10 000	−2.78%	0.78%
$Q4$–200_5	16 977	159	12 837	135	217	12 906	12 888	135	12 870	−0.40%	0.00%
$Q4$–200_6	14 665	149	11 747	127	243	14 493	11 668	128	14 993	0.68%	−0.78%
$Q4$–200_7	15 201	149	11 283	125	181	10 729	11 449	126	10 157	−1.45%	−0.79%
$Q4$–200_8	15 886	153	12 612	133	235	14 013	12 721	132	13 826	−0.86%	0.76%
$Q4$–200_9	16 841	156	12 776	136	192	11 408	12 832	135	10 767	−0.44%	0.74%
$Q4$–200_10	16 211	156	11 275	127	170	10 050	11 376	126	9715	−0.89%	0.79%
$Q4$–300_1	24 396	221	18 451	189	90	7969	18 346	189	8079	0.57%	0.00%
$Q4$–300_2	24 625	230	18 842	193	102	9006	18 725	193	8927	0.62%	0.00%
$Q4$–300_3	24 873	237	18 969	200	100	8864	19 312	199	8780	−1.78%	0.50%
$Q4$–300_4	25 047	239	18 447	210	75	6624	18 444	211	6568	0.02%	−0.47%
$Q4$–300_5	23 727	223	18 246	190	86	7614	18 523	190	7715	−1.50%	0.00%
$Q4$–300_6	25 591	222	20 130	190	84	7403	20 084	190	7814	0.23%	0.00%
$Q4$–300_7	24 883	224	18 785	191	97	8508	18 743	190	8558	0.22%	0.53%
$Q4$–300_8	22 914	229	16 846	193	77	6795	16 754	192	6995	0.55%	0.52%
$Q4$–300_9	25 096	229	19 023	190	91	7988	19 199	189	8153	−0.92%	0.53%
$Q4$–300_10	23 629	229	17 960	192	108	9487	18 179	194	9492	−1.20%	−1.03%
$Q4$–400_1	31 241	295	23 419	247	52	6068	23 460	247	6159	−0.17%	0.00%
$Q4$–400_2	30 679	309	21 775	258	41	4688	22 003	259	4720	−1.04%	−0.39%
$Q4$–400_3	32 284	298	24 751	254	41	4662	24 962	254	4538	−0.85%	0.00%
$Q4$–400_4	33 245	302	24 415	250	49	5588	24 371	250	5598	0.18%	0.00%
$Q4$–400_5	31 333	297	23 967	251	48	5523	23 875	251	5651	0.39%	0.00%
$Q4$–400_6	31 333	304	24 325	264	53	6093	24 226	263	6181	0.41%	0.38%
$Q4$–400_7	31 911	295	24 727	255	46	5354	24 477	255	5686	1.02%	0.00%
$Q4$–400_8	32 825	297	25 298	252	48	5547	25 330	252	5571	−0.13%	0.00%
$Q4$–400_9	32 163	303	24 377	255	42	4758	24 512	255	4702	−0.55%	0.00%
$Q4$–400_10	31 203	303	23 416	248	39	4471	23 717	248	4359	−1.27%	0.00%
$Q4$–500_1	40 288	383	29 817	332	25	3474	30 037	333	3399	−0.73%	−0.30%
$Q4$–500_2	38 828	378	29 501	330	25	3552	29 499	331	3692	0.01%	−0.30%
$Q4$–500_3	39 364	367	29 170	310	33	4605	2949	309	4744	−1.11%	0.32%
$Q4$–500_4	41 534	388	32 308	335	32	4492	32 411	333	4465	−0.32%	0.60%
$Q4$–500_5	41 481	379	31 602	324	30	4184	31 978	323	4130	−1.18%	0.31%
$Q4$–500_6	39 690	374	29 774	316	31	4355	29 870	317	4410	−0.32%	−0.32%
$Q4$–500_7	40 895	385	30 841	329	31	4351	30 994	328	4329	−0.49%	0.30%
$Q4$–500_8	39 994	374	31 781	322	32	4496	31 940	321	4593	−0.50%	0.31%
$Q4$–500_9	41 384	387	30 578	319	33	4604	30 806	319	4682	−0.74%	0.00%
$Q4$–500_10	39 419	378	30 123	323	36	5065	30 232	323	5192	−0.36%	0.00%
AVG.	24 161.20	227.40	18 385.90	193.40	224.50	10 469.20	18 468.30	193.40	10 388.20	−0.48%	0.05%

Table A.14
Results for the datasets $Q20$–100, $Q20$–200, $Q20$–300, $Q20$–400, and $Q20$–500 for the CI–MR setting.

Dataset	z_1	R_1	z_{DRP}	R_{DRP}	Diversif.	DRP iter.	z_{RDR}	R_{RDR}	RDR iter.	DEV_z	DEV_R
$Q20$–100_1	3905	26	3010	20	70	2043	3017	19	1856	−0.23%	5.26%
$Q20$–100_2	4103	27	3070	21	76	2219	3073	21	1896	−0.10%	0.00%
$Q20$–100_3	4742	29	3460	23	73	2141	3450	23	2033	0.29%	0.00%
$Q20$–100_4	4144	26	3142	20	62	1786	3133	19	1635	0.29%	5.26%
$Q20$–100_5	4141	26	3246	21	74	2164	3222	21	2047	0.74%	0.00%
$Q20$–100_6	4560	28	3576	23	61	1778	3549	22	1682	0.76%	4.55%
$Q20$–100_7	4035	25	2894	18	66	1916	2859	18	1896	1.22%	0.00%
$Q20$–100_8	4360	28	3246	21	60	1731	3204	21	1756	1.31%	0.00%
$Q20$–100_9	4071	27	3198	22	64	1839	3202	23	1714	−0.12%	−4.35%
$Q20$–100_10	3451	23	2458	17	77	2240	2463	17	2066	−0.20%	0.00%
$Q20$–200_1	6269	41	4996	33	27	1469	4994	33	1365	0.04%	0.00%
$Q20$–200_2	6427	41	4451	31	22	1188	4457	31	1129	−0.13%	0.00%
$Q20$–200_3	6919	44	4906	32	21	1144	5006	35	1163	−2.00%	−8.57%
$Q20$–200_4	6761	45	4477	33	21	1140	4533	32	982	−1.24%	3.13%
$Q20$–200_5	7270	45	4627	32	24	1310	4658	32	1221	−0.67%	0.00%
$Q20$–200_6	6542	43	4411	31	24	1327	4499	31	1182	−1.96%	0.00%
$Q20$–200_7	6342	41	4504	32	21	1152	4458	32	1119	1.03%	0.00%
$Q20$–200_8	6587	42	4788	32	24	1300	4756	32	1190	0.67%	0.00%
$Q20$–200_9	6928	43	4717	33	19	1028	4899	33	1017	−3.72%	0.00%
$Q20$–200_10	6629	42	4347	31	22	1161	4393	32	1127	−1.05%	−3.13%
$Q20$–300_1	9598	59	6471	45	10	770	6638	45	734	−2.52%	0.00%
$Q20$–300_2	9435	58	6674	46	10	731	6697	45	706	−0.34%	2.22%
$Q20$–300_3	10 398	65	6769	47	10	715	6806	48	786	−0.54%	−2.08%
$Q20$–300_4	9794	62	6765	49	9	648	6614	47	642	2.28%	4.26%
$Q20$–300_5	9328	58	6775	45	9	629	6858	46	602	−1.21%	−2.17%
$Q20$–300_6	10 412	65	7335	49	9	670	7292	48	715	0.59%	2.08%
$Q20$–300_7	9604	60	7016	47	10	740	6996	46	689	0.29%	2.17%
$Q20$–300_8	9416	59	6260	45	9	670	6282	45	682	−0.35%	0.00%
$Q20$–300_9	9350	58	6921	46	10	724	7069	47	690	−2.09%	−2.13%
$Q20$–300_10	9419	60	6747	47	10	747	6856	48	708	−1.59%	−2.08%
$Q20$–400_1	11 413	71	8160	56	5	406	8142	57	411	0.22%	−1.75%
$Q20$–400_2	11 229	70	7849	56	4	354	7809	55	347	0.51%	1.82%
$Q20$–400_3	12 773	76	8707	58	5	345	8910	58	341	−2.28%	0.00%
$Q20$–400_4	12 382	77	8909	60	5	392	8877	60	370	0.36%	0.00%
$Q20$–400_5	11 378	71	8419	56	4	366	8655	57	364	−2.73%	−1.75%
$Q20$–400_6	12 305	77	8424	58	5	420	8447	58	409	−0.27%	0.00%
$Q20$–400_7	12 346	76	8745	59	5	384	8888	59	398	−1.61%	0.00%
$Q20$–400_8	13 211	81	8971	58	4	379	8870	59	380	1.14%	−1.69%
$Q20$–400_9	11 520	71	8562	57	4	341	8479	58	369	0.98%	−1.72%
$Q20$–400_10	12 130	76	8124	58	4	351	8428	58	353	−3.61%	0.00%
$Q20$–500_1	14 000	88	10 657	73	3	240	10 511	74	251	1.39%	−1.35%
$Q20$–500_2	13 969	86	10 097	71	3	262	9906	71	268	1.93%	0.00%
$Q20$–500_3	14 316	90	10 342	71	3	300	10 259	70	295	0.81%	1.43%
$Q20$–500_4	14 693	91	10 926	73	3	262	10 944	73	271	−0.16%	0.00%
$Q20$–500_5	14 119	86	10 966	73	3	259	10 915	73	283	0.47%	0.00%
$Q20$–500_6	13 689	84	10 422	71	3	269	10 619	71	270	−1.86%	0.00%
$Q20$–500_7	14 072	87	10 983	73	3	261	10 576	73	298	3.85%	0.00%
$Q20$–500_8	15 156	94	10 936	72	3	249	11 173	74	259	−2.12%	−2.70%
$Q20$–500_9	14 726	91	10 665	71	3	270	10 347	71	322	3.07%	0.00%
$Q20$–500_10	14 393	89	10 548	71	3	279	10 536	71	306	0.11%	0.00%
AVG.	9375.20	58.60	6733.40	45.70	21.60	910.20	6744.50	45.80	871.90	−0.21%	−0.07%

Table A.15
Results for the datasets $Q20$–100, $Q20$–200, $Q20$–300, $Q20$–400, and $Q20$–500 for the CI–SR setting.

Dataset	z_I	R_I	z_{DRP}	R_{DRP}	Diversif.	DRP iter.	z_{RDR}	R_{RDR}	RDR iter.	DEV_z	DEV_R
$Q20$–100_1	3905	26	3348	21	862	25 788	3404	22	23 796	−1.65%	−4.55%
$Q20$–100_2	4103	27	3329	22	950	28 461	3384	23	26 748	−1.63%	−4.35%
$Q20$–100_3	4742	29	3734	24	975	29 212	3662	23	27 693	1.97%	4.35%
$Q20$–100_4	4144	26	3483	22	830	24 850	3475	21	21 005	0.23%	4.76%
$Q20$–100_5	4141	26	3474	22	1002	30 031	3475	22	27 535	−0.03%	0.00%
$Q20$–100_6	4560	28	3690	22	776	23 221	3907	24	21 554	−5.55%	−8.33%
$Q20$–100_7	4035	25	3388	21	902	26 987	3302	21	28 023	2.60%	0.00%
$Q20$–100_8	4360	28	3416	22	841	25 167	3521	23	23 340	−2.98%	−4.35%
$Q20$–100_9	4071	27	3345	23	833	24 923	3411	23	23 568	−1.93%	0.00%
$Q20$–100_10	3451	23	2772	18	859	25 727	2712	18	26 774	2.21%	0.00%
$Q20$–200_1	6269	41	5373	35	197	11 732	5344	35	12 230	0.54%	0.00%
$Q20$–200_2	6427	41	5071	33	178	10 634	5154	34	9926	−1.61%	−2.94%
$Q20$–200_3	6919	44	5375	36	186	11 034	5656	36	10 623	−4.97%	0.00%
$Q20$–200_4	6761	45	4954	35	168	9971	5082	34	9708	−2.52%	2.94%
$Q20$–200_5	7270	45	5171	34	196	11 606	5450	36	11 747	−5.12%	−5.56%
$Q20$–200_6	6542	43	4808	33	196	11 663	5131	34	10 938	−6.30%	−2.94%
$Q20$–200_7	6342	41	4832	34	179	10 657	5040	35	10 296	−4.13%	−2.86%
$Q20$–200_8	6587	42	5325	34	174	10 333	5269	33	10 498	1.06%	3.03%
$Q20$–200_9	6928	43	5512	36	163	9662	5554	36	9585	−0.76%	0.00%
$Q20$–200_10	6629	42	4837	33	168	9963	5106	34	9531	−5.27%	−2.94%
$Q20$–300_1	9598	59	6948	46	92	8102	7239	47	7735	−4.02%	−2.13%
$Q20$–300_2	9435	58	7261	48	86	7547	7561	48	7196	−3.97%	0.00%
$Q20$–300_3	10 398	65	7507	50	88	7757	7631	49	7628	−1.62%	2.04%
$Q20$–300_4	9794	62	7232	49	75	6603	7811	52	6262	−7.41%	−5.77%
$Q20$–300_5	9328	58	7257	47	76	6650	7316	48	6533	−0.81%	−2.08%
$Q20$–300_6	10 412	65	7873	50	77	6818	8128	52	7245	−3.14%	−3.85%
$Q20$–300_7	9604	60	7361	48	84	7420	7538	49	6740	−2.35%	−2.04%
$Q20$–300_8	9416	59	6794	47	77	6712	7261	49	6670	−6.43%	−4.08%
$Q20$–300_9	9350	58	7627	48	81	7205	7802	50	7309	−2.24%	−4.00%
$Q20$–300_10	9419	60	7263	48	90	7949	7762	50	7387	−6.43%	−4.00%
$Q20$–400_1	11 413	71	8568	57	52	6086	8943	59	5883	−4.19%	−3.39%
$Q20$–400_2	11 229	70	8253	57	47	5457	8743	59	5086	−5.60%	−3.39%
$Q20$–400_3	12 773	76	8759	58	47	5370	9464	60	5257	−7.45%	−3.33%
$Q20$–400_4	12 382	77	9518	62	49	5699	9730	62	5368	−2.18%	0.00%
$Q20$–400_5	11 378	71	9011	58	46	5360	9170	60	5707	−1.73%	−3.33%
$Q20$–400_6	12 305	77	8732	59	57	6568	8910	61	6459	−2.00%	−3.28%
$Q20$–400_7	12 346	76	9238	61	48	5599	9467	61	5588	−2.42%	0.00%
$Q20$–400_8	13 211	81	9617	62	50	5821	9699	61	5696	−0.85%	1.64%
$Q20$–400_9	11 520	71	8783	58	46	5263	8906	59	5092	−1.38%	−1.69%
$Q20$–400_10	12 130	76	8832	60	49	5657	9222	62	5235	−4.23%	−3.23%
$Q20$–500_1	14 000	88	10 928	75	23	3287	11 227	76	3102	−2.66%	−1.32%
$Q20$–500_2	13 969	86	10 737	72	25	3465	10 740	71	3265	−0.03%	1.41%
$Q20$–500_3	14 316	90	10 508	71	26	3746	10 840	72	3766	−3.06%	−1.39%
$Q20$–500_4	14 693	91	11 206	74	26	3601	11 453	74	3529	−2.16%	0.00%
$Q20$–500_5	14 119	86	11 268	74	26	3618	11 383	75	3452	−1.01%	−1.33%
$Q20$–500_6	13 689	84	10 725	70	26	3637	11 204	73	3729	−4.28%	−4.11%
$Q20$–500_7	14 072	87	10 875	74	25	3611	11 439	75	3503	−4.93%	−1.33%
$Q20$–500_8	15 156	94	11 490	73	25	3568	11 855	76	3637	−3.08%	−3.95%
$Q20$–500_9	14 726	91	10 780	72	28	3906	11 169	72	3848	−3.48%	0.00%
$Q20$–500_10	14 393	89	10 992	72	29	4058	10 925	73	4219	0.61%	−1.37%
AVG.	9375.2	58.6	7143.6	47.2	244.2	10 755.2	7351.5	48	10 344.9	−2.61%	−1.66%

Table A.16
Results for the datasets $Q20$–100, $Q20$–200, $Q20$–300, $Q20$–400, and $Q20$–500 for the SI–MR setting.

Dataset	z_I	R_I	z_{DRP}	R_{DRP}	Diversif.	DRP iter.	z_{RDR}	R_{RDR}	RDR iter.	DEV_z	DEV_R
$Q20$–100_1	5754	47	3018	20	81	2348	2997	19	2237	0.70%	5.26%
$Q20$–100_2	5499	46	3073	21	84	2445	3074	21	2247	−0.03%	0.00%
$Q20$–100_3	6911	52	3470	23	82	2404	3451	23	2383	0.55%	0.00%
$Q20$–100_4	5533	45	3143	20	71	2031	3139	20	1868	0.13%	0.00%
$Q20$–100_5	5715	44	3257	21	90	2640	3203	21	2544	1.69%	0.00%
$Q20$–100_6	5850	44	3557	23	74	2154	3561	23	2005	−0.11%	0.00%
$Q20$–100_7	5877	48	2913	18	87	2553	2852	18	2452	2.14%	0.00%
$Q20$–100_8	5565	44	3194	20	73	2114	3209	20	2095	−0.47%	0.00%
$Q20$–100_9	5561	46	3194	23	73	2131	3202	23	2076	−0.25%	0.00%
$Q20$–100_10	4564	38	2433	17	88	2570	2424	17	2489	0.37%	0.00%
$Q20$–200_1	9946	84	4922	33	25	1349	4971	33	1313	−0.99%	0.00%
$Q20$–200_2	8880	80	4555	31	20	1060	4499	31	1039	1.24%	0.00%
$Q20$–200_3	10 274	85	4796	33	23	1234	4919	33	1215	−2.50%	0.00%
$Q20$–200_4	10 016	85	4504	32	20	1066	4532	33	1032	−0.62%	−3.03%
$Q20$–200_5	10 300	84	4552	31	25	1319	4680	32	1256	−2.74%	−3.13%
$Q20$–200_6	9141	81	4417	31	23	1205	4510	32	1174	−2.06%	−3.13%
$Q20$–200_7	9931	91	4548	33	21	1112	4478	32	1109	1.56%	3.13%
$Q20$–200_8	10 369	85	4804	33	24	1264	4764	32	1167	0.84%	3.13%
$Q20$–200_9	9680	76	4886	34	20	1058	4793	33	1067	1.94%	3.03%
$Q20$–200_10	10 161	94	4322	31	21	1143	4417	33	1115	−2.15%	−6.06%
$Q20$–300_1	15 656	126	6611	45	9	662	6536	45	695	1.15%	0.00%
$Q20$–300_2	15 223	127	6758	46	9	668	6887	45	598	−1.87%	2.22%
$Q20$–300_3	16 214	134	6872	47	10	697	6892	48	674	−0.29%	−2.08%
$Q20$–300_4	14 794	126	6692	48	8	539	6811	48	566	−1.75%	0.00%
$Q20$–300_5	14 394	119	6714	45	9	602	6728	44	596	−0.21%	2.27%
$Q20$–300_6	16 642	128	7328	48	9	616	7240	48	628	1.22%	0.00%
$Q20$–300_7	16 579	130	6892	46	10	665	7040	46	605	−2.10%	0.00%
$Q20$–300_8	13 797	123	6184	44	8	572	6156	46	597	0.45%	−4.35%
$Q20$–300_9	16 301	132	6942	46	9	656	6905	45	660	0.54%	2.22%
$Q20$–300_10	14 639	125	6678	46	10	721	6707	47	697	−0.43%	−2.13%
$Q20$–400_1	19 280	160	8249	57	6	440	8315	57	435	−0.79%	0.00%
$Q20$–400_2	18 227	167	7782	57	5	385	7810	57	389	−0.36%	0.00%
$Q20$–400_3	19 794	159	8648	58	5	367	8829	57	377	−2.05%	1.75%
$Q20$–400_4	20 078	161	8742	59	5	414	8809	61	421	−0.76%	−3.28%
$Q20$–400_5	19 623	165	8463	57	5	394	8622	57	383	−1.84%	0.00%
$Q20$–400_6	19 060	163	8485	58	5	459	8617	59	449	−1.53%	−1.69%
$Q20$–400_7	19 133	159	8710	59	5	397	8870	60	420	−1.80%	−1.67%
$Q20$–400_8	20 412	167	9266	62	5	401	9017	59	398	2.76%	5.08%
$Q20$–400_9	20 094	165	8544	58	5	375	8402	58	371	1.69%	0.00%
$Q20$–400_10	19 553	173	8393	59	5	375	8291	59	402	1.23%	0.00%
$Q20$–500_1	23 527	202	10 362	73	3	221	10 840	75	236	−4.41%	−2.67%
$Q20$–500_2	22 330	197	9826	70	3	249	10 133	71	255	−3.03%	−1.41%
$Q20$–500_3	23 892	207	10 199	69	3	282	10 442	72	282	−2.33%	−4.17%
$Q20$–500_4	23 788	198	10 936	73	3	257	10 785	72	266	1.40%	1.39%
$Q20$–500_5	24 374	191	10 832	73	3	246	11 024	72	253	−1.74%	1.39%
$Q20$–500_6	24 622	205	10 808	72	3	240	10 428	70	304	3.64%	2.86%
$Q20$–500_7	24 543	206	10 515	72	3	284	10 942	73	273	−3.90%	−1.37%
$Q20$–500_8	24 959	207	10 863	71	3	279	10 812	71	290	0.47%	0.00%
$Q20$–500_9	25 615	213	10 572	70	3	283	10 653	71	279	−0.76%	−1.41%
$Q20$–500_10	23 933	205	10 500	71	3	282	10 431	71	311	0.66%	0.00%
AVG.	14 932.1	124.8	6718.5	45.7	23.9	964.6	6753.0	45.9	939.9	−0.35	−0.16

Table A.17
Results for the datasets $Q20$–100, $Q20$–200, $Q20$–300, $Q20$–400, and $Q20$–500 for the SI–SR setting.

Dataset	z_I	R_I	z_{DRP}	R_{DRP}	Diversif.	DRP iter.	z_{RDR}	R_{RDR}	RDR iter.	DEV_z	DEV_R
$Q20$–100_1	5754	47	3362	22	904	27 055	3286	21	27 582	2.31%	4.76%
$Q20$–100_2	5499	46	3241	22	928	27 765	3369	22	26 725	−3.80%	0.00%
$Q20$–100_3	6911	52	3739	24	953	28 542	3722	24	27 259	0.46%	0.00%
$Q20$–100_4	5533	45	3346	21	794	23 754	3518	22	23 233	−4.89%	−4.55%
$Q20$–100_5	5715	44	3414	22	1047	31 353	3475	22	28 316	−1.76%	0.00%
$Q20$–100_6	5850	44	3738	23	757	22 637	3875	25	23 393	−3.54%	−8.00%
$Q20$–100_7	5877	48	3188	21	1007	30 146	3371	21	25 487	−5.43%	0.00%
$Q20$–100_8	5565	44	3429	22	843	25 216	3599	24	22 738	−4.72%	−8.33%
$Q20$–100_9	5561	46	3403	24	840	25 122	3431	23	22 922	−0.82%	4.35%
$Q20$–100_10	4564	38	2699	19	950	28 452	2732	18	26 877	−1.21%	5.56%
$Q20$–200_1	9946	84	5298	35	272	16 197	5413	35	15 035	−2.12%	0.00%
$Q20$–200_2	8880	80	4896	33	223	13 224	5043	33	12 436	−2.91%	0.00%
$Q20$–200_3	10 274	85	5524	36	237	14 122	5548	36	13 703	−0.43%	0.00%
$Q20$–200_4	10 016	85	4951	34	219	13 002	5167	35	12 132	−4.18%	−2.86%
$Q20$–200_5	10 300	84	4965	34	267	15 876	5366	35	14 118	−7.47%	−2.86%
$Q20$–200_6	9141	81	4919	33	256	15 259	4931	32	14 328	−0.24%	3.13%
$Q20$–200_7	9931	91	4874	34	225	13 378	4904	34	13 384	−0.61%	0.00%
$Q20$–200_8	10 369	85	5111	33	234	13 873	5414	35	13 546	−5.60%	−5.71%
$Q20$–200_9	9680	76	5151	34	215	12 767	5571	35	11 563	−7.54%	−2.86%
$Q20$–200_10	10 161	94	4936	33	222	13 212	5187	34	11 971	−4.84%	−2.94%
$Q20$–300_1	15 656	126	7133	46	99	8694	7060	46	8564	1.03%	0.00%
$Q20$–300_2	15 223	127	7348	47	93	8138	7462	47	7896	−1.53%	0.00%
$Q20$–300_3	16 214	134	7371	50	101	8864	7613	50	8569	−3.18%	0.00%
$Q20$–300_4	14 794	126	7369	52	82	7226	7542	53	7798	−2.29%	−1.89%
$Q20$–300_5	14 394	119	7191	48	93	8190	7287	47	7186	−1.32%	2.13%
$Q20$–300_6	16 642	128	7761	50	90	7857	8243	52	8147	−5.85%	−3.85%
$Q20$–300_7	16 579	130	7292	49	99	8666	7621	50	8406	−4.32%	−2.00%
$Q20$–300_8	13 797	123	6772	46	86	7494	7103	48	7633	−4.66%	−4.17%
$Q20$–300_9	16 301	132	7713	49	98	8670	7606	49	8642	1.41%	0.00%
$Q20$–300_10	14 639	125	7420	50	101	8934	7717	51	8633	−3.85%	−1.96%
$Q20$–400_1	19 280	160	8465	56	51	5863	8866	59	6059	−4.52%	−5.08%
$Q20$–400_2	18 227	167	8199	58	46	5331	8386	59	5336	−2.23%	−1.69%
$Q20$–400_3	19 794	159	8972	59	45	5125	9414	61	5156	−4.70%	−3.28%
$Q20$–400_4	20 078	161	9180	61	50	5810	9510	62	5619	−3.47%	−1.61%
$Q20$–400_5	19 623	165	8957	59	48	5523	8945	58	5355	0.13%	1.72%
$Q20$–400_6	19 060	163	8947	61	53	6104	9282	61	6005	−3.61%	0.00%
$Q20$–400_7	19 133	159	9288	61	49	5643	9122	59	5457	1.82%	3.39%
$Q20$–400_8	20 412	167	9815	63	48	5576	9534	62	5591	2.95%	1.61%
$Q20$–400_9	20 094	165	8711	58	45	5150	9104	59	4939	−4.32%	−1.69%
$Q20$–400_10	19 553	173	8820	61	45	5172	8898	61	5092	−0.88%	0.00%
$Q20$–500_1	23 527	202	10 957	76	22	2999	11 184	77	3028	−2.03%	−1.30%
$Q20$–500_2	22 330	197	10 713	73	23	3227	10 604	72	3343	1.03%	1.39%
$Q20$–500_3	23 892	207	10 397	71	27	3844	10 521	72	3795	−1.18%	−1.39%
$Q20$–500_4	23 788	198	11 068	74	26	3573	11 444	74	3416	−3.29%	0.00%
$Q20$–500_5	24 374	191	11 152	74	26	3636	11 204	75	3602	−0.46%	−1.33%
$Q20$–500_6	24 622	205	10 796	71	26	3677	10 877	70	3690	−0.74%	1.43%
$Q20$–500_7	24 543	206	11 096	74	26	3679	11 238	75	3762	−1.26%	−1.33%
$Q20$–500_8	24 959	207	11 526	75	26	3560	11 716	76	3647	−1.62%	−1.32%
$Q20$–500_9	25 615	213	11 015	73	27	3808	11 045	72	3749	−0.27%	1.39%
$Q20$–500_10	23 933	205	10 776	72	28	3982	11 045	73	4022	−2.44%	−1.37%
AVG.	14 932.1	124.8	7128.1	47.5	261.4	11 699.3	7282.3	47.9	11 177.7	−2.30	−0.85

References

Alfandari, L., Ljubić, I., De Melo da Silva, M., 2022. A tailored benders decomposition approach for last-mile delivery with autonomous robots. European J. Oper. Res. 299 (2), 510–525.

Alonso Raponso, M., Grosso, M., Mourtzouchou, A., Krause, J., Duboz, A., Ciuffo, B., 2022. Economic implications of a connected and automated mobility in Europe. Res. Transport. Econ. 92, 101072.

Alverhed, E., Hellgren, S., Isaksson, H., Olsson, L., Palmqvist, H., Flodén, J., 2024. Autonomous last-mile delivery robots: A literature review. Eur. Transp. Res. Rev. 16 (4).

Archetti, C., Savelsbergh, M., Speranza, M., 2016. The vehicle routing problem with occasional drivers. European J. Oper. Res. 254 (2), 472–480.

Azcuy, I., Agatz, N., Giesen, R., 2021. Designing integrated urban delivery systems using public transport. Transp. Res. E 156, 102525.

Bailey, R., 2016. Ground drones will beat air drones. https://reason.com/2016/02/24/ground-drones-will-beat-air-drones/. (Last Accessed on: 30 June 2023).

Behiri, W., Belmokhtar-Berraf, S., Chu, C., 2018. Urban freight transport using passenger rail network: Scientific issues and quantitative analysis. Transp. Res. E 115, 227–245.

Bosse, A., Ulmer, M., Manni, E., Mattfeld, D., 2023. Dynamic priority rules for combining on-demand passenger transportation and transportation of goods. European J. Oper. Res. 309 (1), 399–408.

Boysen, N., Schwerdfeger, S., Weidinger, F., 2018. Scheduling last-mile deliveries with truck-based autonomous robots. European J. Oper. Res. 271 (3), 1085–1099.

Carracedo, D., Mostofi, H., 2022. Electric cargo bikes in urban areas: A new mobility option for private transportation. Transp. Res. Interdiscip. Perspect. 16, 100705.

Chen, C., Demir, E., Huang, Y., Qiu, R., 2021. The adoption of self-driving delivery robots in last mile logistics. Transp. Res. E 146, 102214.

Cochrane, K., Saxe, S., Roorda, M., Shalaby, A., 2017. Moving freight on public transit: Best practices, challenges, and opportunities. Int. J. Sustain. Transp. 11 (2), 120–132.

Contardo, C., Martinelli, R., 2014. A new exact algorithm for the multi-depot vehicle routing problem under capacity and route length constraints. Discrete Optim. 12, 129–146.

Delle Donne, D., Alfandari, L., Archetti, C., Ljubić, I., 2023. Freight-on-transit for urban last-mile deliveries: A strategic planning approach. Transp. Res. B 169, 53–81.

Duarte, N., Sánchez-Oro, J., Todosijević, R., 2018. Variable neighborhood descent. In: Handbook of Heuristics. Springer International Publishing, pp. 341–367.

Elbert, R., Rentschler, J., 2022. Freight on urban public transportation: A systematic literature review. Res. Transp. Bus. Manag. 45, 100679, Urban logistics: From research to implementation.

Ermagan, U., Yildiz, B., Salman, S., 2023. Machine learning-enhanced column generation approach for express shipments with autonomous robots and public transportation. Available at SSRN 4471292.

FedEx, 2020. Meet Roxo, the FedEx SameDay Bot. https://www.fedex.com/en-cw/about/sustainability/our-approach/roxo-delivery-robot.html. (Last Accessed on: 30 June 2023).

Figliozzi, M., 2020. Carbon emissions reductions in last mile and grocery deliveries utilizing air and ground autonomous vehicles. Transp. Res. D 85, 102443.

Galkin, A., Schlosser, T., Galkina, O., Hodáková, D., Cápayová, S., 2019. Investigating using urban public transport for freight deliveries. Transp. Res. Procedia 39, 64–73, 3rd International Conference "Green Cities – Green Logistics for Greener Cities", Szczecin, 13-14 September 2018.

Geronimo, A., 2023. Aramex tests drone and robot delivery service in Dubai. https://www.itp.net/emergent-tech/aramex-tests-drone-and-robot-delivery-service-in-dubai. (Last Accessed on: 30 June 2023).

Grabenschweiger, J., Doerner, K., Hartl, R., Savelsbergh, M., 2021. The vehicle routing problem with heterogeneous locker boxes. CEJOR Cent. Eur. J. Oper. Res. 29, 113–142.

Heimfarth, A., Ostermeier, M., Hübner, A., 2022. A mixed truck and robot delivery approach for the daily supply of customers. European J. Oper. Res. 303 (1), 401–421.

Hörsting, L., Cleophas, C., 2023. Scheduling shared passenger and freight transport on a fixed infrastructure. European J. Oper. Res. 306 (3), 1158–1169.

Kapser, S., Abdelrahman, M., Bernecker, T., 2021. Autonomous delivery vehicles to fight the spread of Covid-19 – How do men and women differ in their acceptance? Transp. Res. A 148, 183–198.

Kızıl, K., Yıldız, B., 2023. Public transport-based crowd-shipping with backup transfers. Transp. Sci. 57 (1), 174–196.

Kloster, K., Moeini, M., Vigo, D., Wendt, O., 2023. The multiple traveling salesman problem in presence of drone- and robot-supported packet stations. European J. Oper. Res. 305 (2), 630–643.

Kunze, O., 2016. Replicators, ground drones and crowd logistics a vision of urban logistics in the year 2030. Transp. Res. Procedia 19, 286–299, Transforming Urban Mobility. mobil.TUM 2016. International Scientific Conference on Mobility and Transport. Conference Proceedings.

Le, T., Stathopoulos, A., Van Woensel, T., Ukkusuri, S., 2019. Supply, demand, operations, and management of crowdshipping services: A review and empirical evidence. Transp. Res. C 103, 83–103.

Lemardelé, C., Estrada, M., Pagès, L., Bachofner, M., 2021. Potentialities of drones and ground autonomous delivery devices for last-mile logistics. Transp. Res. E 149, 102325.

Li, B., Krushinsky, D., Reijers, H., Van Woensel, T., 2014. The share-a-ride problem: People and parcels sharing taxis. European J. Oper. Res. 238 (1), 31–40.

Macrina, G., Di Puglia Pugliese, L., Guerriero, F., Laporte, G., 2020. Drone-aided routing: A literature review. Transp. Res. C 120, 102762.

Martí, R., Pardalos, P., Resende, M.G.C., 2018. Handbook of heuristics. In: Mathematics and Statistics, Reference Module Computer Science and Engineering.

Masson, R., Trentini, A., Lehuédé, F., Malhéné, N., Péton, O., Tlahig, H., 2017. Optimization of a city logistics transportation system with mixed passengers and goods. EURO J. Transport. Logist. 6 (1), 81–109.

Mourad, A., Puchinger, J., Chu, C., 2019. A survey of models and algorithms for optimizing shared mobility. Transp. Res. B 123, 323–346.

Mourad, A., Puchinger, J., Van Woensel, T., 2021. Integrating autonomous delivery service into a passenger transportation system. Int. J. Prod. Res. 59 (7), 2116–2139.

Pani, A., Mishra, S., Golias, M., Figliozzi, M., 2020. Evaluating public acceptance of autonomous delivery robots during COVID-19 pandemic. Transp. Res. D 89, 102600.

Pisinger, D., Ropke, S., 2010. Large neighborhood search. In: Gendreau, M., Potvin, J.-Y. (Eds.), Handbook of Metaheuristics. Springer US, Boston, MA, pp. 399–419.

Raghunatha, A., Lindkvist, E., Thollander, P., Hansson, E., Jonsson, G., 2023. Critical assessment of emissions, costs, and time for last-mile goods delivery by drones versus trucks. Sci. Rep. 13 (1), 11814.

Ranieri, L., Digiesi, S., Silvestri, B., Roccotelli, M., 2018. A review of last mile logistics innovations in an externalities cost reduction vision. Sustainability 10 (3), 1–18.

Rong Cheng, Y., Nielsen, O., 2023. Integrated people-and-goods transportation systems: From a literature review to a general framework for future research. Transp. Rev. 43 (5), 997–1020.

Rosenkrantz, D., Stearns, R., Lewis, P., 1977. An analysis of several heuristics for the traveling salesman problem. SIAM J. Comput. 6 (3), 563–581.

Sehlleier, F., Imboden, A., Gota, S., Hagge, K., 2017. Green freight and logistics in the context of Sustainable Development Goals (SDGs). Tenth Regional EST Forum in Asia.

Solomon, M., 1987. Algorithms for the vehicle routing and scheduling problems with time windows constraints. Oper. Res. 35, 254–262.
Srinivas, S., Ramachandiran, S., Rajendran, S., 2022. Autonomous robot-driven deliveries: A review of recent developments and future directions. Transp. Res. E 165, 102834.
Starship, 2020. Starship's self-driving robot. http://www.starship.xyz. (Last Accessed on: 30 June 2023).
Statista, 2023. Ecommerce report 2023. https://www.statista.com/study/42335/ecommerce-report/. (Last Accessed on: 30 June 2023).
United Nations, 2022. The 17 goals. https://sdgs.un.org/goals. (Last Accessed on: 30 June 2023).
Vincent, J., Gartenberg, C., 2019. Here's Amazon's new transforming Prime Air delivery drone. https://www.theverge.com/2019/6/5/18654044/amazon-prime-air-delivery-drone-new-design-safety-transforming-flight-video. (Last Accessed on: 30 June 2023).
Yu, S., Puchinger, J., Sun, S., 2022. Van-based robot hybrid pickup and delivery routing problem. European J. Oper. Res. 298 (3), 894–914.